

# Non-leptonic weak processes in spin-one color superconducting quark matter

Xinyang Wang,<sup>1</sup> Hossein Malekzadeh,<sup>2,3</sup> and Igor A. Shovkovy<sup>1,4,\*</sup>

<sup>1</sup>*Department of Physics, Arizona State University, Tempe, Arizona 85287, USA*

<sup>2</sup>*Institut für Theoretische Physik, Westfälische Wilhelms-Universität Münster, D-48149 Münster, Germany*

<sup>3</sup>*Physik Department, Technische Universität München, D-85748 Garching, Germany*

<sup>4</sup>*Department of Applied Sciences and Mathematics,  
Arizona State University, Mesa, Arizona 85212, USA*

(Dated: December 19, 2009)

The non-leptonic weak processes  $s + u \rightarrow u + d$  and  $u + d \rightarrow s + u$  are known to dominate the dissipation mechanism responsible for the viscosity of strange quark matter in its normal phase. The rates of such processes remain unknown for many color superconducting phases of quark matter. In this paper, we partially fill up the gap by calculating the difference of the rates of the two non-leptonic weak processes in four transverse spin-one color superconducting phases of quark matter (slightly) out of  $\beta$ -equilibrium. The four phases studied are the color-spin locked phase, the polar phase, the planar phase and the  $A$ -phase. In the limit of vanishing color superconducting gap, we reproduce the known results in the normal phase. In the general case, the rates are suppressed relative to the normal phase. The degree of the suppression is determined by the structure of the gap function in momentum space, which in turn is determined by the pairing pattern of quarks. At low temperatures, the rate is dominated by the ungapped modes. In this limit, the strongest suppression of the rate occurs in the color-spin-locked phase, and the weakest is in the polar phase and the  $A$ -phase.

PACS numbers: 12.38.Mh, 12.15.Ji, 95.30.Cq, 97.60.Jd

## I. INTRODUCTION

The interior of neutron stars is made of very dense baryonic matter. Currently our knowledge regarding the actual state of such matter is incomplete. One commonly accepted hypotheses is that the densest regions inside neutron stars are made of quark matter [1]. Moreover, such quark matter may be a color superconductor [2, 3]. (For reviews on color superconductivity see for example Refs. [4, 5, 6, 7, 8, 9, 10, 11, 12].) From the viewpoint of basic research, it is of fundamental importance to test this hypothesis empirically.

The way to test the idea regarding the presence of quark matter inside stars is to make predictions regarding physics processes that affect observable features of stars and then test them against the stellar data. One class of physics properties that are substantially modified by the presence of color superconducting quark matter is related to the rates of weak processes. Such processes, for example, affect the cooling rates [13] and the suppression of the rotational (r-mode) instabilities [14] in stars. The latter in particular is determined by the viscous properties of dense matter [15].

Theoretically, the ground state of baryonic matter at very high density corresponds to the color-flavor-locked (CFL) phase of quark matter [16]. In this phase, quarks of all three colors and all three flavors participate in spin-zero Cooper pairing on equal footing. The rates of the weak processes and some of their effects on the physical

properties of the CFL phase of quark matter have been discussed in Refs. [17, 18, 19, 20, 21].

With decreasing the density, the CFL phase should break up. This is due to the disruptive effects of a large difference between the masses of the strange quark and the light (up and down) quarks [22]. Such a difference leads to a mismatch between the Fermi momenta of quarks and, therefore, spoils the “democratic” pairing of the CFL phase. When the CFL phase breaks up, another type of spin-zero color superconductivity, the so-called two-flavor color superconducting (2SC) phase [23], can still be possible. In the 2SC phase, strange quarks do not participate in pairing. Also, up and down quarks of one color remain unpaired. Some weak processes in the 2SC phase and their effects on the physical properties have been studied in Refs. [24, 25].

It is important to mention that matter inside stars is neutral (at least on average) and in  $\beta$ -equilibrium. Enforcing these two conditions affects the pairing between quarks and may disrupt the usual formation of cross-flavor spin-zero Cooper pairs [22]. In this case, the ground state of matter can be in other forms, for example, such as stable variants of crystalline [26], gapless [27, 28], or other exotic phases [29, 30]. When spin-zero pairing cannot occur, the ground state can be in one of the spin-one color superconducting phases, in which same flavor quarks combine to form Cooper pairs [31, 32, 33, 34, 35].

Compared to the spin-zero case, the energy gap in spin-one color superconductors is likely to be about two orders of magnitude smaller. This means that the actual value of the gap may be somewhere in the range from 0.01 MeV to 1 MeV. It appears that even such relatively small gaps can substantially affect the cooling rate of a quark

---

\*Electronic address: igor.shovkovy@asu.edu

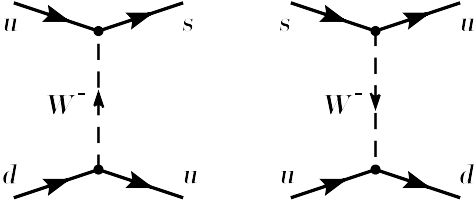


FIG. 1: Feynman diagrams of the non-leptonic weak processes

star [36]. By the same token, such gaps can strongly modify the rates of the non-leptonic weak processes and, thus, affect the viscosity of stellar quark matter.

The bulk viscosity in the normal phase of three-flavor quark matter is usually dominated by the non-leptonic weak processes [37, 38, 39, 40, 41, 42]. (The corresponding processes are diagrammatically shown in Fig. 1.) It was argued in Ref. [43], however, that the interplay between the Urca and non-leptonic processes may be rather involved even in the normal phase of quark matter. Indeed, because of the resonance-like dynamics responsible for the bulk viscosity and because of a subtle interference between the two types of the weak processes, a larger rate of the non-leptonic processes may not automatically mean its dominant role. In fact, it was shown that the contributions of the two types of weak processes are not separable and that, at low frequencies relevant for some pulsars, taking into account the Urca processes may substantially modify the result [43].

Currently it remains unknown how a similar interplay between the two types of weak processes is realized in spin-one color superconducting phases. Primarily, this is because the rates of the non-leptonic weak processes in the corresponding phases have not been calculated. (Note that the rates of the Urca processes in several spin-one color superconducting phases were obtained in Refs. [36, 44].) The purpose of this paper is to study the corresponding non-leptonic rates.

The rest of the paper is organized as follows. The derivation of a general expression for the non-leptonic rate, based on the Kadanoff-Baym formalism [46], is presented in the next section. The structure of the quark propagators in spin-one color superconducting phases is described in Subsec. II A. This is used in Subsec. II B to derive the imaginary part of the  $W$ -boson polarization tensor, which is the key ingredient in the expression for the rate. The net rate of the  $d$ -quark production (i.e., the difference of the rates of  $s+u \rightarrow u+d$  and  $u+d \rightarrow s+u$ ) in the case of a small deviation from chemical equilibrium is obtained in Sec. III. There we also present the numerical results for each of the following spin-one color superconducting phases: the CSL phase (Subsec. III A), the polar phase (Subsec. III B), the A-phase (Subsec. III C), and the planar phase (Subsec. III D). In Sec. IV, we discuss the main results and their physical meaning. Two Appendices at the end of the paper contain some details,

used in the derivation of the rate.

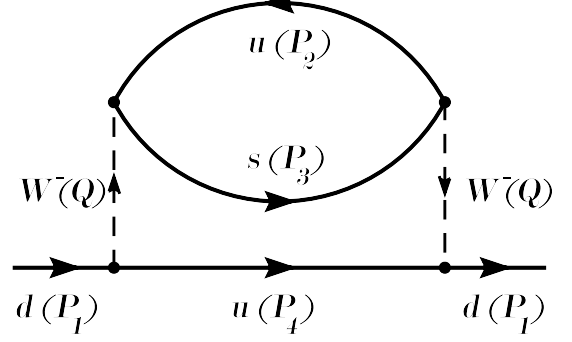


FIG. 2: Feynman diagram for the  $d$ -quark self-energy. The particle four-momenta are shown in parenthesis next to the particle names.

## II. FORMALISM

In order to calculate the rates of the non-leptonic processes, we use the same approach as in Refs. [25, 36, 43, 44, 45]. It is based on the Kadanoff-Baym formalism [46]. The starting point of the analysis is the general Kadanoff-Baym equation for the Green functions (propagators) of the down (or strange) quarks. After applying the conventional gradient expansion close to equilibrium, we derive the following kinetic equation for the  $d$ -quark Green function:

$$i \frac{\partial}{\partial t} \text{Tr}[\gamma_0 S_d^<(P_1)] = -\text{Tr}[S_d^>(P_1) \Sigma^<(P_1) - \Sigma^>(P_1) S_d^<(P_1)]. \quad (1)$$

Here we denote the quark four-momenta by capital letters, e.g.,  $P = (p_0, \mathbf{p})$ , where  $p_0$  is the energy and  $\mathbf{p}$  is the three-momentum. The structure of the quark Green's functions  $S^<(P_1)$  and  $S^>(P_1)$  in spin-one color superconducting phases will be discussed in the next subsection. To leading order, the quark self-energies  $\Sigma^<(P_1)$  and  $\Sigma^>(P_1)$  are given by the Feynman diagram in Fig. 2. This translates into the following explicit expression:

$$\Sigma^{<,>}(P_1) = \frac{i}{M_W^4} \int \frac{d^4 P_4}{(2\pi)^4} \Gamma_{ud,-}^\mu S_u^{<,>}(P_4) \Gamma_{ud,+}^\nu \Pi_{\mu\nu}^{>,<}(Q), \quad (2)$$

where, by definition,  $M_W$  and  $Q = P_1 - P_4$  are the mass and the four-momentum of the  $W$ -boson, respectively. (Note that the large hierarchy between the  $W$ -boson mass and a typical momentum transfer  $Q \lesssim 1$  MeV justifies the approximation in which the  $W$ -boson propagator is replaced by  $1/M_W^2$ .) As seen from the diagram in Fig. 2, the expression for the polarization tensor of the  $W$ -boson is given by

$$\Pi_{\mu\nu}^{<, >}(Q) = -i \int \frac{d^4 P_2}{(2\pi)^4} \text{Tr} \left[ \Gamma_{us,+}^\mu S_s^{>,<}(P_2 + Q) \Gamma_{us,-}^\nu S_u^{<,>}(P_2) \right]. \quad (3)$$

In the Nambu-Gorkov notation used here, the explicit form of the (tree-level) vertices for the weak processes  $d \leftrightarrow u + W^-$  and  $s \leftrightarrow u + W^-$  reads [25]

$$\Gamma_{ud/us,\pm}^\mu = \frac{e V_{ud/us}}{2\sqrt{2} \sin \theta_W} \begin{pmatrix} \gamma^\mu (1 - \gamma^5) \tau_{ud/us,\pm} & 0 \\ 0 & -\gamma^\mu (1 + \gamma^5) \tau_{ud/us,\mp} \end{pmatrix}. \quad (4)$$

These are given in terms of the elements of the Cabibbo-Kobayashi-Maskawa matrix  $V_{ud}$  and  $V_{us}$ , and the weak mixing angle  $\theta_W$ . By construction, the  $\tau$ -matrices operate in flavor space ( $u, d, s$ ) and have the following form:

$$\tau_{ud,+} \equiv \begin{pmatrix} 0 & 1 & 0 \\ 0 & 0 & 0 \\ 0 & 0 & 0 \end{pmatrix}, \quad \tau_{ud,-} \equiv \begin{pmatrix} 0 & 0 & 0 \\ 1 & 0 & 0 \\ 0 & 0 & 0 \end{pmatrix}, \quad \tau_{us,+} \equiv \begin{pmatrix} 0 & 0 & 1 \\ 0 & 0 & 0 \\ 0 & 0 & 0 \end{pmatrix}, \quad \tau_{us,-} \equiv \begin{pmatrix} 0 & 0 & 0 \\ 0 & 0 & 0 \\ 1 & 0 & 0 \end{pmatrix}. \quad (5)$$

By making use of Eqs. (1) and (2), the kinetic equation takes the following form:

$$i \frac{\partial}{\partial t} \text{Tr}[\gamma_0 S_d^<(P_1)] = -\frac{i}{M_W^4} \int \frac{dP_4}{(2\pi)^4} \text{Tr} \left[ S_d^>(P_1) \Gamma_{ud,-}^\mu S_u^<(P_4) \Gamma_{ud,+}^\nu \Pi_{\mu\nu}^>(Q) - \Gamma_{ud,-}^\mu S_u^>(P_4) \Gamma_{ud,+}^\nu S_d^<(P_1) \Pi_{\mu\nu}^<(Q) \right]. \quad (6)$$

The physical meaning of the expression on the left hand side of this equation is the time derivative of the  $d$ -quark distribution function. By integrating this over the complete phase space, we obtain the net rate of the  $d$ -quark production:

$$\Gamma_d \equiv -\frac{i}{4} \frac{\partial}{\partial t} \int \frac{dP_1}{(2\pi)^4} \text{Tr}[\gamma_0 S_d^<(P_1)]. \quad (7)$$

Then, by making use of the kinetic equation (1), we derive

$$\begin{aligned} \Gamma_d &= \frac{i}{4M_W^4} \int \frac{d^4 P_1}{(2\pi)^4} \int \frac{dP_4}{(2\pi)^4} \\ &\times \left[ \text{Tr} \left( S_d^>(P_1) \Gamma_{ud,-}^\mu S_u^<(P_4) \Gamma_{ud,+}^\nu \right) \Pi_{\mu\nu}^>(Q) \right. \\ &\left. - \text{Tr} \left( \Gamma_{ud,-}^\mu S_u^>(P_4) \Gamma_{ud,+}^\nu S_d^<(P_1) \right) \Pi_{\mu\nu}^<(Q) \right]. \quad (8) \end{aligned}$$

This rate should be non-vanishing only if the rates of the two non-leptonic weak processes  $u + s \rightarrow d + u$  and  $d + u \rightarrow u + s$  differ. In  $\beta$ -equilibrium, in particular, the latter two should be equal and the net rate of the  $d$ -quark production should vanish. The corresponding state of equilibrium in dense quark matter is reached when the chemical potentials of all three quark flavors are equal, i.e.,  $\mu_u = \mu_d = \mu_s$ . (For simplicity, here it is assumed that all three quark flavors are approximately massless and, therefore, that the electrical neutrality of quark matter is achieved without the need for the electrons.)

When the system is forced out of equilibrium, e.g., during the density oscillations caused by the collective modes of stellar matter, small deviations from  $\beta$ -equilibrium are induced. For our purposes, the corresponding state can

be described by the following set of the chemical potentials:  $\mu_u = \mu_d = \mu$  and  $\mu_s = \mu + \delta\mu$ , where  $\delta\mu$  is a small parameter that characterizes the magnitude of the departure from the equilibrium state. Out of equilibrium, the net production of  $d$ -quarks may be nonzero. For example, if  $\delta\mu > 0$  ( $\delta\mu < 0$ ) the system has a deficit (an excess) of the down quarks and an excess (a deficit) of the strange quarks. Then, one of the weak processes, i.e.,  $u + s \rightarrow d + u$  ( $d + u \rightarrow u + s$ ), will start to dominate over the other in order to restore the equilibrium. The net rate of the  $d$ -quark (or equivalently  $s$ -quark) production characterizes how quickly this happens.

In order to calculate the net rate of  $d$ -quark production, however, one needs to know the explicit structure of the quark propagators in the specific spin-one color superconducting phases. The knowledge of the quark propagators is also needed for the calculation of the polarization tensors  $\Pi_{\mu\nu}^<(Q)$  and  $\Pi_{\mu\nu}^>(Q)$ . These are discussed in the next two subsections.

### A. Quark propagator in a spin-one color superconductor

In general, Cooper pairs in spin-one color superconducting phases are given by diquarks in a color antitriplet (antisymmetric) and spin triplet (symmetric) state. Depending on a specific color-spin structure, which is determined by the alignments of the antitriplet in color space and the triplet in spin (coordinate) space, many inequivalent color superconducting phases may form.

Each phase is unambiguously specified by the structure of the gap matrix, which is commonly written in the

following form [32]:

$$\Phi(P)^+ = \sum_{e=\pm} \phi^e(P) \mathcal{M}_{\mathbf{p}} \Lambda_{\mathbf{p}}^e, \quad (9)$$

where  $\phi^e(P)$  is the gap function. The Dirac matrices  $\Lambda_{\mathbf{p}}^e \equiv (1 + e\gamma_0 \boldsymbol{\gamma} \cdot \hat{\mathbf{p}})/2$ , with  $e = \pm$ , are the projectors onto the positive and negative energy states. The color structure of  $\Phi(P)^+$  is determined by

$$\mathcal{M}_{\mathbf{p}} = \sum_{i,j=1}^3 J^i \Delta_{ij} \left[ \hat{p}^j \cos \theta + \gamma_{\perp}^j \sin \theta \right]. \quad (10)$$

where  $(J^i)^{jk} = -i\epsilon^{ijk}$  are the antisymmetric matrices in color space,  $\hat{\mathbf{p}} \equiv \mathbf{p}/p$  is the unit vector in the direction of the quasiparticle three-momentum  $\mathbf{p}$ , and  $\gamma_{\perp}^j \equiv \gamma^j - \hat{p}^j(\boldsymbol{\gamma} \cdot \hat{\mathbf{p}})$ . The explicit form of the  $3 \times 3$  matrix  $\Delta_{ij}$  and the value of the angular parameter  $\theta$  determine specific phases of superconducting matter. Among them, there is a number of inert and noninert spin-one phases [35], which are naturally characterized by the continuous and discrete symmetries preserved in the ground state.

In the two special cases,  $\theta = 0$  and  $\theta = \pi/2$ , the corresponding phases are called longitudinal and transverse, respectively. In this paper we focus on the transverse phases ( $\theta = \pi/2$ ), in which only quarks of the opposite chiralities pair and which have lower free energies than the longitudinal phases [32]. To further constrain the large number of possibilities, we concentrate only on the following four most popular ones: the color-spin locked phase (CSL), the A-phase, the polar phase and the planar phase.

The structure of the matrices  $\Delta_{ij}$  and  $\mathcal{M}_{\mathbf{p}}$  for the mentioned four phases are quoted in the first two rows of Tab. I (for more details see Refs. [32]). In the corresponding ground states, the original symmetry  $SU(3)_c \times SO(3)_J \times U(1)_{\text{em}}$  of one-flavor quark matter breaks down to [31, 32, 33, 34, 35]

$$\begin{aligned} \widetilde{SO}(3)_J & \quad (\text{CSL}), \\ SU(2)_c \times \widetilde{SO}(2)_J \times \tilde{U}(1)_{\text{em}} & \quad (\text{A-phase}), \\ SU(2)_c \times SO(2)_J \times \tilde{U}(1)_{\text{em}} & \quad (\text{polar}), \\ \widetilde{SO}(2)_J \times \tilde{U}(1)_{\text{em}} & \quad (\text{planar}), \end{aligned}$$

respectively.

In spin-one color superconductors, there is no cross-flavor pairing and, therefore, the quark propagator is diagonal in flavor space, i.e.,

$$S(P) = \text{diag}[S_u(P), S_d(P), S_s(P)]. \quad (11)$$

The Nambu-Gorkov structure of each flavor-diagonal element is given by

$$S_f^{<,>}(P) = \begin{pmatrix} G_{f,+}^{<,>}(P) & F_{f,-}^{<,>}(P) \\ F_{f,+}^{<,>}(P) & G_{f,-}^{<,>}(P) \end{pmatrix}, \quad (12)$$

where  $f = u, d, s$ . The normal (diagonal) and anomalous (off-diagonal) components of the Nambu-Gorkov propagator have the following structure [32]:

$$G_{f,\pm}^{<,>}(P) = \gamma_0 \Lambda_{\mathbf{p}}^{\mp} \sum_r \mathcal{P}_{\mathbf{p},r}^{\pm} G_{\pm,r,f}^{<,>}(P), \quad (13)$$

$$F_{f,+}^{<,>}(P) = -\gamma_0 \mathcal{M}_{\mathbf{p}} \gamma_0 \sum_{e,r} \mathcal{P}_{\mathbf{p},r}^+ \Lambda_{\mathbf{p}}^e F_{+,r,f}^{<,>}(P), \quad (14)$$

$$F_{f,-}^{<,>}(P) = -\mathcal{M}_{\mathbf{p}}^{\dagger} \sum_{e,r} \mathcal{P}_{\mathbf{p},r}^- \Lambda_{\mathbf{p}}^e F_{-,r,f}^{<,>}(P). \quad (15)$$

Here,  $r$  labels different quasiparticle excitations in color-superconducting quark matter. The matrices  $\mathcal{P}_{\mathbf{p},r}^{\pm}$  and  $\mathcal{P}_{\mathbf{p},r}^+$  are the projectors onto the subspaces spanned by the eigenvectors of  $\mathcal{M}_{\mathbf{p}} \mathcal{M}_{\mathbf{p}}^{\dagger}$  and  $\gamma^0 \mathcal{M}_{\mathbf{p}}^{\dagger} \mathcal{M}_{\mathbf{p}} \gamma^0$ , respectively. The explicit form of the projectors for each phase can be found in Ref. [36]. It should be noted that both matrices  $\mathcal{M}_{\mathbf{p}} \mathcal{M}_{\mathbf{p}}^{\dagger}$  and  $\gamma^0 \mathcal{M}_{\mathbf{p}}^{\dagger} \mathcal{M}_{\mathbf{p}} \gamma^0$  have the same set of eigenvalues  $\lambda_{\mathbf{p},r}$ ,

$$\mathcal{M}_{\mathbf{p}} \mathcal{M}_{\mathbf{p}}^{\dagger} \equiv \sum_r \lambda_{\mathbf{p},r} \mathcal{P}_{\mathbf{p},r}^-, \quad (16)$$

$$\gamma^0 \mathcal{M}_{\mathbf{p}}^{\dagger} \mathcal{M}_{\mathbf{p}} \gamma^0 \equiv \sum_r \lambda_{\mathbf{p},r} \mathcal{P}_{\mathbf{p},r}^+. \quad (17)$$

The list of all eigenvalues as well as their degeneracies are given in the last three rows of Tab. I. Each of the eigenvalues determines a quark quasiparticle with the following dispersion relation:

$$\epsilon_{\mathbf{p},r,f} = \sqrt{(p - \mu_f)^2 + |\phi|^2 \lambda_{\mathbf{p},r,f}}. \quad (18)$$

The separate components of the propagators in subspaces spanned by the eigenvectors, see Eqs. (13), (14) and (15), can be conveniently rewritten in terms of the corresponding distribution functions  $f(\epsilon_{p,r,f})$  and the Bogoliubov coefficients  $B_{\mathbf{p},r,f}^{\pm}$ , i.e.,

$$G_{\pm,r,f}^{>}(P) = -2\pi i \sum_{e=\pm} B_{\mathbf{p},r,f}^{\pm e} f(e\epsilon_{p,r,f}) \delta(p_0 \pm \mu_f - e\epsilon_{p,r,f}), \quad (19)$$

$$G_{\pm,r,f}^{<}(P) = -2\pi i \sum_{e=\pm} B_{\mathbf{p},r,f}^{\pm e} f(-e\epsilon_{p,r,f}) \delta(p_0 \pm \mu_f - e\epsilon_{p,r,f}), \quad (20)$$

$$F_{\pm,r,f}^{>}(P) = 2\pi i \frac{\phi}{2\epsilon_{p,r,f}} \sum_{e=\pm} e f(e\epsilon_{p,r,f}) \delta(p_0 \mp \mu_f - e\epsilon_{p,r,f}), \quad (21)$$

$$F_{\pm,r,f}^{<}(P) = 2\pi i \frac{\phi}{2\epsilon_{p,r,f}} \sum_{e=\pm} e f(-e\epsilon_{p,r,f}) \delta(p_0 \pm \mu_f - e\epsilon_{p,r,f}). \quad (22)$$

The Bogoliubov coefficients and the fermion distribution function are defined as follows:

$$B_{\mathbf{p},r,f}^e = \frac{1}{2} - e \frac{p - \mu_f}{2\epsilon_{\mathbf{p},r,f}}, \quad (23)$$

$$f(\epsilon) = \frac{1}{\exp(\frac{\epsilon}{T}) + 1}. \quad (24)$$

	CSL phase	planar phase	polar phase	A-phase
$\Delta_{ij}$	$\delta_{ij}$	$\delta_{i1}\delta_{j1} + \delta_{i2}\delta_{j2}$	$\delta_{i3}\delta_{j3}$	$\delta_{i3}(\delta_{j1} + i\delta_{j2})$
$\mathcal{M}_{\mathbf{p}}$	$\mathbf{J} \cdot \boldsymbol{\gamma}_{\perp}(\hat{\mathbf{p}})$	$J_1\gamma_{\perp,1}(\hat{\mathbf{p}}) + J_2\gamma_{\perp,2}(\hat{\mathbf{p}})$	$J_3\gamma_{\perp,3}(\hat{\mathbf{p}})$	$J_3[\gamma_{\perp,1}(\hat{\mathbf{p}}) + i\gamma_{\perp,2}(\hat{\mathbf{p}})]$
$\lambda_{\mathbf{p},1} (n_1)$	2 (8)	$1 + \cos^2 \theta_{\mathbf{p}}$ (8)	$\sin^2 \theta_{\mathbf{p}}$ (8)	$(1 +  \cos \theta_{\mathbf{p}} )^2$ (4)
$\lambda_{\mathbf{p},2} (n_2)$	0 (4)	0 (4)	0 (4)	$(1 -  \cos \theta_{\mathbf{p}} )^2$ (4)
$\lambda_{\mathbf{p},3} (n_3)$	—	—	—	0 (4)

TABLE I: Matrices  $\Delta_{ij}$  and  $\mathcal{M}_{\mathbf{p}}$  as well as the eigenvalues  $\lambda_{\mathbf{p},r}$  with the corresponding degeneracies  $n_r$  in four spin-one color superconducting phases. The angle between  $\mathbf{p}$  and the  $z$ -axis is denoted by  $\theta_{\mathbf{p}}$ .

[Note that  $f(-\epsilon) = 1 - f(\epsilon)$ .] The quark propagators in Eq. (12) can now be used to derive the general expressions for  $\Pi_{\mu\nu}^{<}(Q)$  and  $\Pi_{\mu\nu}^{>}(Q)$ . This is done in the next subsection. The results are then used to calculate the rate  $\Gamma_d$  in Eq. (8).

### B. $W$ -boson polarization tensor

The  $W$ -boson polarization tensor is given in terms of the quark propagators in Eq. (3). By taking into account the Nambu-Gorkov and flavor structure of the weak interaction vertices in Eq. (4), as well as the quark propagator in Eq. (12), we derive

$$\begin{aligned} \Pi_{\mu\nu}^{<,>}(Q) = & -\frac{ie^2V_{us}^2}{8\sin^2\theta_W} \int \frac{d^4P_2}{(2\pi)^4} \\ & \times \text{Tr} \left[ \gamma^\mu (1 - \gamma^5) G_{s,+}^{>,<}(P_3) \gamma^\nu (1 - \gamma^5) G_{u,+}^{<,>}(P_2) \right. \\ & \left. + \gamma^\mu (1 + \gamma^5) G_{u,-}^{>,<}(P_3) \gamma^\nu (1 + \gamma^5) G_{s,-}^{<,>}(P_2) \right], \quad (25) \end{aligned}$$

where we introduced the notation  $P_3 \equiv P_2 + Q$ . Note that the anomalous (off-diagonal) elements of the Nambu-

Gorkov propagators dropped out from the result. This is the consequence of the electric charge conservation. In calculations, this comes about as a result of the specific flavor structure of the weak interaction vertices in Eq. (4). One can further simplify the result for the polarization tensor in Eq. (25) by noticing that the two terms on the right hand side are equal. From physical viewpoint, this is related to the fact that the two terms are the charge-conjugate contributions of each other. After taking this into, we arrive at the following expression for the polarization tensor:

$$\begin{aligned} \Pi_{\mu\nu}^{<,>}(Q) = & -\frac{ie^2V_{us}^2}{4\sin^2\theta_W} \int \frac{d^4P_2}{(2\pi)^4} \text{Tr} \left[ \gamma^\mu (1 - \gamma^5) \right. \\ & \left. \times G_{s,+}^{>,<}(P_3) \gamma^\nu (1 - \gamma^5) G_{u,+}^{<,>}(P_2) \right]. \quad (26) \end{aligned}$$

Then, by using the explicit structure of the normal components of the  $u$ - and  $s$ -quark propagators, defined in Eq. (13), we obtain

$$\Pi_{\mu\nu}^{<,>}(Q) = -\frac{ie^2V_{us}^2}{4\sin^2\theta_W} \int \frac{d^4P_2}{(2\pi)^4} \text{Tr} \left[ \gamma^\mu (1 - \gamma^5) \gamma_0 \Lambda_{\mathbf{p}_3}^- \sum_{r_3} \mathcal{P}_{\mathbf{p}_3,r_3}^+ G_{+,r_3,s}^{>,<}(P_3) \gamma^\nu (1 - \gamma^5) \gamma_0 \Lambda_{\mathbf{p}_2}^- \sum_{r_2} \mathcal{P}_{\mathbf{p}_2,r_2}^+ G_{+,r_2,u}^{<,>}(P_2) \right]. \quad (27)$$

This can be rewritten in an equivalent form as

$$\Pi_{\mu\nu}^{<,>} = -\frac{ie^2V_{us}^2}{4\sin^2\theta_W} \int \frac{d^4P_2}{(2\pi)^4} \sum_{r_2,r_3} \mathcal{T}_{\mu\nu}^{r_3 r_2}(\hat{\mathbf{p}}_3, \hat{\mathbf{p}}_2) G_{+,r_3,s}^{>,<}(P_3) G_{+,r_2,u}^{<,>}(P_2). \quad (28)$$

where, by definition, the tensor  $\mathcal{T}_{\mu\nu}^{rr'}(\hat{\mathbf{p}}, \hat{\mathbf{p}}')$  is given by the following trace (in color and Dirac spaces):

$$\mathcal{T}_{\mu\nu}^{rr'}(\hat{\mathbf{p}}, \hat{\mathbf{p}}') = \text{Tr} [\gamma^\mu (1 - \gamma^5) \gamma_0 \Lambda_{\mathbf{p}}^- \mathcal{P}_{\mathbf{p},r}^+ \gamma^\nu (1 - \gamma^5) \gamma_0 \Lambda_{\mathbf{p}'}^- \mathcal{P}_{\mathbf{p}',r'}^+]. \quad (29)$$

This trace was calculated for each of the four spin-one color superconducting phases in Ref. [36]. For convenience, the corresponding results are also quoted in Appendix A.

Finally, by making use of Eqs. (19) and (20), we arrive at the following expression for the  $W$ -boson polarization



tensor:

$$\begin{aligned} \Pi_{\mu\nu}^{<, >} &= \frac{i\pi e^2 V_{us}^2}{2 \sin^2 \theta_W} \int \frac{d^3 \mathbf{p}_2}{(2\pi)^3} \sum_{r_2, r_3, e_1, e_2} \mathcal{T}_{\mu\nu}^{r_3 r_2}(\hat{\mathbf{p}}_3, \hat{\mathbf{p}}_2) B_{\mathbf{p}_3, r_3, s}^{e_1} B_{\mathbf{p}_2, r_2, u}^{e_2} \\ &\times f(\pm e_1 \epsilon_{\mathbf{p}_3, r_3, s}) f(\mp e_2 \epsilon_{\mathbf{p}_2, r_2, u}) \delta(q_0 + \delta\mu - e_1 \epsilon_{\mathbf{p}_3, r_3, s} + e_2 \epsilon_{\mathbf{p}_2, r_2, u}). \end{aligned} \quad (30)$$

Here we denote  $\delta\mu \equiv \mu_s - \mu_u$  and assume that the upper (lower) sign corresponds to  $\Pi^<$  ( $\Pi^>$ ). It should be mentioned that one of the  $\delta$ -functions was used to perform the integration over  $p_{2,0}$ .

### III. CALCULATION OF THE RATE

In this section we derive a general expression for the net rate of the  $d$ -quark production in spin-one color superconducting quark matter close to chemical equilibrium. The corresponding rate is formally defined by Eq. (8). By making use of the quark propagators and the  $W$ -boson polarization tensor, derived in the previous section, we obtain

$$\begin{aligned} \Gamma_d &= \frac{ie^2 V_{ud}^2}{16 M_W^4 \sin^2 \theta_W} \int \frac{d^4 P_1}{(2\pi)^4} \int \frac{d^4 P_4}{(2\pi)^4} \sum_{r_1, r_4} \mathcal{T}_{r_4 r_1}^{\mu\nu}(\hat{\mathbf{p}}_4, \hat{\mathbf{p}}_1) \\ &\times \left[ G_{+, r_1, d}^>(P_1) G_{+, r_4, u}^<(P_4) \Pi_{\mu\nu}^>(Q) - G_{+, r_4, u}^>(P_4) G_{+, r_1, d}^<(P_1) \Pi_{\mu\nu}^<(Q) \right]. \end{aligned} \quad (31)$$

where we used the following results for the traces:

$$\text{Tr} \left( S_d^>(P_1) \Gamma_{ud, -}^\mu S_u^<(P_4) \Gamma_{ud, +}^\nu \right) = \frac{e^2 V_{ud}^2}{4 \sin^2 \theta_W} \sum_{r_1, r_4} \mathcal{T}_{r_4 r_1}^{\mu\nu}(\hat{\mathbf{p}}_4, \hat{\mathbf{p}}_1) G_{+, r_1, d}^>(P_1) G_{+, r_4, u}^<(P_4), \quad (32)$$

$$\text{Tr} \left( \Gamma_{ud, -}^\mu S_u^>(P_4) \Gamma_{ud, +}^\nu S_d^<(P_1) \right) = \frac{e^2 V_{ud}^2}{4 \sin^2 \theta_W} \sum_{r_1, r_4} \mathcal{T}_{r_4 r_1}^{\mu\nu}(\hat{\mathbf{p}}_4, \hat{\mathbf{p}}_1) G_{+, r_4, u}^>(P_4) G_{+, r_1, d}^<(P_1). \quad (33)$$

As in the calculation of the polarization tensor, the anomalous (off-diagonal) Nambu-Gorkov components of quark propagators did not contribute to these traces. This is the consequence of the specific flavor structure of the weak interaction vertices (4).

After making use of Eqs. (19), (20) and (30), we obtain

$$\begin{aligned} \Gamma_d &= 2^7 \pi^4 G_F^2 V_{ud}^2 V_{us}^2 \sum_{r_1 r_2 r_3 r_4} \sum_{e_1 e_2 e_3 e_4} \int \frac{d^3 \mathbf{p}_1}{(2\pi)^3} \frac{d^3 \mathbf{p}_2}{(2\pi)^3} \frac{d^3 \mathbf{p}_3}{(2\pi)^3} \frac{d^3 \mathbf{p}_4}{(2\pi)^3} (1 - \hat{\mathbf{p}}_1 \cdot \hat{\mathbf{p}}_2)(1 - \hat{\mathbf{p}}_3 \cdot \hat{\mathbf{p}}_4) \omega_{r_4 r_1}(\hat{\mathbf{p}}_4, \hat{\mathbf{p}}_1) \omega_{r_3 r_2}(\hat{\mathbf{p}}_3, \hat{\mathbf{p}}_2) \\ &\times B_{\mathbf{p}_1, r_1, d}^{e_1} B_{\mathbf{p}_2, r_2, u}^{e_2} B_{\mathbf{p}_3, r_3, s}^{e_3} B_{\mathbf{p}_4, r_4, u}^{e_4} \delta(\mathbf{p}_1 + \mathbf{p}_2 - \mathbf{p}_3 - \mathbf{p}_4) \delta(e_1 \epsilon_{\mathbf{p}_1, r_1, d} + e_2 \epsilon_{\mathbf{p}_2, r_2, u} - e_3 \epsilon_{\mathbf{p}_3, r_3, s} - e_4 \epsilon_{\mathbf{p}_4, r_4, u} + \delta\mu) \\ &\times [f(e_1 \epsilon_{\mathbf{p}_1, r_1, d}) f(e_2 \epsilon_{\mathbf{p}_2, r_2, u}) f(-e_3 \epsilon_{\mathbf{p}_3, r_3, s}) f(-e_4 \epsilon_{\mathbf{p}_4, r_4, u}) - f(-e_1 \epsilon_{\mathbf{p}_1, r_1, d}) f(-e_2 \epsilon_{\mathbf{p}_2, r_2, u}) f(e_3 \epsilon_{\mathbf{p}_3, r_3, s}) f(e_4 \epsilon_{\mathbf{p}_4, r_4, u})]. \end{aligned} \quad (34)$$

In derivation, we used the definition of the Fermi constant in terms of the  $W$ -boson mass,

$$G_F = \frac{e^2}{4\sqrt{2} \sin^2 \theta_W M_W^2} \quad (35)$$

and the following Lorentz contraction:

$$\begin{aligned} \mathcal{T}_{r_4 r_1}^{\mu\nu}(\hat{\mathbf{p}}_4, \hat{\mathbf{p}}_1) \mathcal{T}_{\mu\nu}^{r_3 r_2}(\hat{\mathbf{p}}_3, \hat{\mathbf{p}}_2) &= 16(1 - \hat{\mathbf{p}}_1 \cdot \hat{\mathbf{p}}_2) \\ &\times (1 - \hat{\mathbf{p}}_3 \cdot \hat{\mathbf{p}}_4) \omega_{r_4 r_1}(\hat{\mathbf{p}}_4, \hat{\mathbf{p}}_1) \omega_{r_3 r_2}(\hat{\mathbf{p}}_3, \hat{\mathbf{p}}_2), \end{aligned} \quad (36)$$

where  $\omega_{rr'}(\hat{\mathbf{p}}, \hat{\mathbf{p}}')$  denotes a color trace that involves a pair of quasiparticles ( $r$  and  $r'$ ) with the given directions of their three-momenta ( $\hat{\mathbf{p}}$  and  $\hat{\mathbf{p}}'$ ) in a specific spin-one color superconducting phase. The corresponding traces for all four phases are listed in Appendix A.

Formally, the expression in Eq. (34) gives the net rate of the  $d$ -quark production in quark matter away from chemical equilibrium. The first term in the brackets describes the production of  $d$ -quarks due to  $s + u \rightarrow u + d$ , while the second one describes the annihilation of  $d$ -quarks due to  $u + d \rightarrow s + u$ .

Here it might be instructive to note that the above expression for the rate  $\Gamma_d$  resembles the general result for the net rate of the  $d$ -quark production in the normal phase of strange quark matter [47]. The key difference comes from the presence of the Bogoliubov coefficients  $B_{\mathbf{p}, r, f}$  and the  $\omega_{rr'}(\hat{\mathbf{p}}, \hat{\mathbf{p}}')$  functions that account for a non-trivial quark structure of the quasiparticles in spin-one color superconductors. Naturally, when such quasi-

particles are the asymptotic states for the weak processes, the amplitude is not the same as in the normal phase.

The degree of departure from  $\beta$ -equilibrium and, thus, the net rate is controlled by the parameter  $\delta\mu = \mu_s - \mu_d$ . When  $\delta\mu = 0$ , the expression in the square brackets of Eq. (34) vanishes and  $\Gamma_d = 0$ . When  $\delta\mu \neq 0$ , on the other hand, one has

$$\Gamma_d \simeq \lambda \delta\mu \quad (37)$$

to leading order in small  $\delta\mu$  [48]. Note that the overall sign was chosen so that  $\lambda$  is positive definite. (Recall that a positive  $\delta\mu$  means an excess of strange quarks, which should drive a net production of  $d$ -quarks, while a negative  $\delta\mu$  means a deficit of strange quarks, which will be produced by annihilating some  $d$ -quarks.)

From the general expression in Eq. (34), we derive

---


$$\begin{aligned} \lambda = & \frac{5\lambda_0}{2^{11}\pi^5\mu^5T^3} \sum_{r_1r_2r_3r_4} \sum_{e_1e_2e_3e_4} \int d^3\mathbf{p}_1 d^3\mathbf{p}_2 d^3\mathbf{p}_3 d^3\mathbf{p}_4 (1 - \hat{\mathbf{p}}_1 \cdot \hat{\mathbf{p}}_2)(1 - \hat{\mathbf{p}}_3 \cdot \hat{\mathbf{p}}_4) \omega_{r_4r_1}(\hat{\mathbf{p}}_4, \hat{\mathbf{p}}_1) \omega_{r_3r_2}(\hat{\mathbf{p}}_3, \hat{\mathbf{p}}_2) \\ & \times B_{\mathbf{p}_1, r_1, d}^{e_1} B_{\mathbf{p}_2, r_2, u}^{e_2} B_{\mathbf{p}_3, r_3, s}^{e_3} B_{\mathbf{p}_4, r_4, u}^{e_4} \delta(\mathbf{p}_1 + \mathbf{p}_2 - \mathbf{p}_3 - \mathbf{p}_4) \delta(e_1\epsilon_{\mathbf{p}_1, r_1, d} + e_2\epsilon_{\mathbf{p}_2, r_2, u} - e_3\epsilon_{\mathbf{p}_3, r_3, s} - e_4\epsilon_{\mathbf{p}_4, r_4, u}) \\ & \times f(-e_1\epsilon_{\mathbf{p}_1, r_1, d}) f(-e_2\epsilon_{\mathbf{p}_2, r_2, u}) f(e_3\epsilon_{\mathbf{p}_3, r_3, s}) f(e_4\epsilon_{\mathbf{p}_4, r_4, u}). \end{aligned} \quad (38)$$

where

$$\lambda_0 = \frac{64G_F^2 V_{ud}^2 V_{us}^2}{5\pi^3} \mu^5 T^2 \quad (39)$$

is the corresponding  $\lambda$ -rate in the normal phase of strange quark matter [47].

### A. Analysis of the rate in CSL phase

Out of the four spin-one color superconducting phases studied in this paper, the CSL phase is special. This is the only phase in which the dispersion relations of quasiparticles are isotropic. As a result, the corresponding rate is the easiest to calculate. In this subsection, we analyze the  $\lambda$ -rate in the CSL phase in detail.

Let us start by noting that the explicit form of the  $\omega_{rr'}(\hat{\mathbf{p}}, \hat{\mathbf{p}}')$ -functions in the CSL phase is given by

$$\omega_{11}(\hat{\mathbf{p}}, \hat{\mathbf{p}}') = 1 + \frac{1}{4}(1 + \hat{\mathbf{p}} \cdot \hat{\mathbf{p}}')^2, \quad (40)$$

$$\omega_{12}(\hat{\mathbf{p}}, \hat{\mathbf{p}}') = \omega_{21}(\hat{\mathbf{p}}, \hat{\mathbf{p}}') = 1 - \frac{1}{4}(1 + \hat{\mathbf{p}} \cdot \hat{\mathbf{p}}')^2, \quad (41)$$

$$\omega_{22}(\hat{\mathbf{p}}, \hat{\mathbf{p}}') = \frac{1}{4}(1 + \hat{\mathbf{p}} \cdot \hat{\mathbf{p}}')^2. \quad (42)$$

(See Appendix A and Ref. [36].) By making use of these expressions and introducing the following notation for the angular integrals:

$$F_{r_1r_2r_3r_4} = \int d\Omega_1 \int d\Omega_2 \int d\Omega_3 \int d\Omega_4 (1 - \hat{\mathbf{p}}_3 \cdot \hat{\mathbf{p}}_4)(1 - \hat{\mathbf{p}}_1 \cdot \hat{\mathbf{p}}_2) \omega_{r_4r_1}(\hat{\mathbf{p}}_4, \hat{\mathbf{p}}_1) \omega_{r_3r_2}(\hat{\mathbf{p}}_3, \hat{\mathbf{p}}_2) \delta(\mathbf{p}_1 + \mathbf{p}_2 - \mathbf{p}_3 - \mathbf{p}_4), \quad (43)$$

we arrive at the following representation for the  $\lambda$ -rate in the CSL phase:

$$\begin{aligned} \lambda^{(\text{CSL})} = & \frac{5\lambda_0\mu^3}{2^{11}\pi^5T^3} \sum_{r_1r_2r_3r_4} \sum_{e_1e_2e_3e_4} \int_0^\infty dp_1 \int_0^\infty dp_2 \int_0^\infty dp_3 \int_0^\infty dp_4 F_{r_1r_2r_3r_4} B_{\mathbf{p}_1, r_1, d}^{e_1} B_{\mathbf{p}_2, r_2, u}^{e_2} B_{\mathbf{p}_3, r_3, s}^{e_3} B_{\mathbf{p}_4, r_4, u}^{e_4} \\ & \times f(-e_1\epsilon_{\mathbf{p}_1, r_1, d}) f(-e_2\epsilon_{\mathbf{p}_2, r_2, u}) f(e_3\epsilon_{\mathbf{p}_3, r_3, s}) f(e_4\epsilon_{\mathbf{p}_4, r_4, u}) \delta(e_1\epsilon_{\mathbf{p}_1, r_1, d} + e_2\epsilon_{\mathbf{p}_2, r_2, u} - e_3\epsilon_{\mathbf{p}_3, r_3, s} - e_4\epsilon_{\mathbf{p}_4, r_4, u}). \end{aligned} \quad (44)$$


---

Here we took into account that, to leading order in inverse powers of  $\mu$ , the absolute values of the quark three-momenta can be approximated by  $\mu$ . In the same approximation, the explicit form of functions  $F_{r_1r_2r_3r_4}$  are given

in Appendix B. All of them are proportional to  $1/\mu^3$ . This factor cancels out with the overall  $\mu^3$  in Eq. (44). In order to perform the remaining numerical integrations, it is convenient to introduce new dimensionless integration

variables  $x_i = (p_i - \mu)/T$  instead of  $p_i$  ( $i = 1, 2, 3, 4$ ). The integration over  $x_4$  is done explicitly by making use of the  $\delta$ -function. The remaining three-dimensional integration is done numerically, using a Monte-Carlo method. One finds that the ratio  $\lambda^{(\text{CSL})}/\lambda_0$  is a function of a single dimensionless ratio,  $\phi/T$ .

Before proceeding to the numerical results, it is instructive to analyze the limiting case of low temperatures (or alternatively very large  $\phi/T$ ). In this limit, only the ungapped  $r = 2$  quasiparticle modes should contribute to the rate. The corresponding contribution is easy to obtain analytically, i.e.,

$$\begin{aligned}\lambda^{(\text{CSL})} &\simeq \frac{\lambda_0 F_{2222}}{\sum_{r_1 r_2 r_3 r_4} F_{r_1 r_2 r_3 r_4}} \\ &= \frac{928}{27027} \lambda_0 \approx 0.034 \lambda_0, \quad \text{for } \frac{\phi}{T} \rightarrow \infty. \quad (45)\end{aligned}$$

The subleading correction to this result is suppressed by an exponentially small factor  $\exp(-\sqrt{2}\phi/T)$ . (Note that  $\sqrt{2}$  in the exponent is connected with the conventional choice of the CSL gap, which is  $\sqrt{2}\phi$  rather than  $\phi$ .)

It might be instructive to mention that the asymptotic value in Eq. (45) is substantially smaller than  $\lambda_0/9$ , which is the corresponding contribution of a single ungapped mode in the normal phase. The additional suppression comes from the functions  $\omega_{22}(\hat{\mathbf{p}}_4, \hat{\mathbf{p}}_1)$  and  $\omega_{22}(\hat{\mathbf{p}}_3, \hat{\mathbf{p}}_2)$  which modify the amplitude of the weak processes with respect to the normal phase. Except for the special case of collinear processes (i.e.,  $\hat{\mathbf{p}}_4$  parallel to  $\hat{\mathbf{p}}_1$  and  $\hat{\mathbf{p}}_3$  parallel to  $\hat{\mathbf{p}}_2$ ), the corresponding  $\omega$ -functions are less than 1, see Eq. (42). Interestingly, this kind of suppression is a unique property of the non-leptonic rates and is not seen in analogous Urca rates because the latter are dominated by the collinear processes [36, 44].

All our numerical results for the  $\lambda$ -rates as a function of  $\phi/T$  are shown in Fig. 3 [49]. In the case of the CSL phase (black points and the interpolating line in Fig. 3), we used the Mathematica's adaptive quasi-Monte-Carlo method to calculate the  $\lambda$ -rate. In order to improve the efficiency of the method, we partitioned the range of integration for each of the three dimensionless integration variables  $x_i = (p_i - \mu)/T$  into several (up to 6) non-overlapping regions. This approach insures that the main contribution, coming from a close neighborhood of the

Fermi sphere, is not lost in the integration over a formally very large phase space.

As seen from Fig. 3, the numerical results smoothly interpolate between the value of the rate in the normal phase  $\lambda_0$  and the asymptotic value of the rate due to the CSL ungapped modes, given by Eq. (45).

## B. Analysis of the rate in polar phase

Unlike the CSL phase, the polar phase is not isotropic. However, it is the simplest one among the other three phases. While the dispersions relations of its quasiparticles depend on the angle  $\theta_{\mathbf{p}}$  between the momentum  $\mathbf{p}$

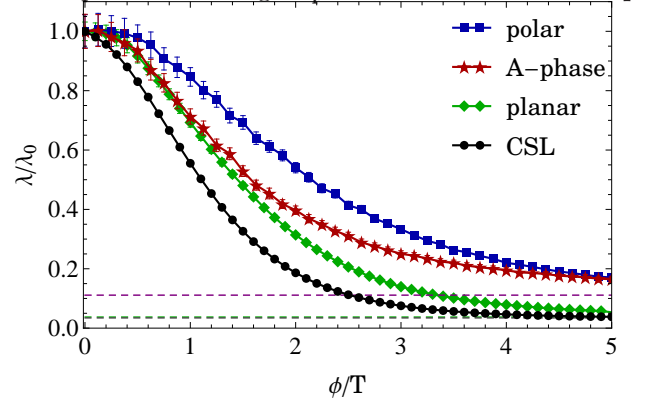


FIG. 3: (Color online) Numerical results for the  $\lambda$ -rate in four different phases of spin-one color superconducting strange quark matter [49]. The error bars show the statistical error estimates in the Monte-Carlo calculation of the rates. The horizontal dashed lines correspond to the contributions of the ungapped modes in the limit of large  $\phi/T$  (or equivalently the limit of low temperatures).

and a fixed  $z$ -direction, its  $\omega_{rr'}(\hat{\mathbf{p}}, \hat{\mathbf{p}}')$ -functions are independent of the quasiparticle momenta, i.e.,

$$\omega_{rr'}(\hat{\mathbf{p}}, \hat{\mathbf{p}}') = n_r \delta_{rr'}, \quad (46)$$

with  $n_1 = 2$  and  $n_2 = 1$ , see Appendix A. Taking this into account, the corresponding  $\lambda$ -rate takes a simple form:

$$\begin{aligned}\lambda^{(\text{polar})} &= \frac{5\lambda_0}{2^{11}\pi^5\mu^5T^3} \sum_{r_1 r_2} n_{r_1} n_{r_2} \sum_{e_1 e_2 e_3 e_4} \int d^3\mathbf{p}_1 d^3\mathbf{p}_2 d^3\mathbf{p}_3 d^3\mathbf{p}_4 (1 - \hat{\mathbf{p}}_1 \cdot \hat{\mathbf{p}}_2)(1 - \hat{\mathbf{p}}_3 \cdot \hat{\mathbf{p}}_4) \delta(\mathbf{p}_1 + \mathbf{p}_2 - \mathbf{p}_3 - \mathbf{p}_4) \\ &\times B_{\mathbf{p}_1, r_1, d}^{e_1} B_{\mathbf{p}_2, r_2, u}^{e_2} B_{\mathbf{p}_3, r_2, s}^{e_3} B_{\mathbf{p}_4, r_1, u}^{e_4} f(-e_1 \epsilon_{\mathbf{p}_1, r_1, d}) f(-e_2 \epsilon_{\mathbf{p}_2, r_2, u}) f(e_3 \epsilon_{\mathbf{p}_3, r_2, s}) f(e_4 \epsilon_{\mathbf{p}_4, r_1, u}) \\ &\times \delta(e_1 \epsilon_{\mathbf{p}_1, r_1, d} + e_2 \epsilon_{\mathbf{p}_2, r_2, u} - e_3 \epsilon_{\mathbf{p}_3, r_2, s} - e_4 \epsilon_{\mathbf{p}_4, r_1, u}). \quad (47)\end{aligned}$$

By making use of the first  $\delta$ -function, we easily perform the integration over  $\mathbf{p}_4$ . We can also perform the integration over one of the remaining polar coordinates. This is possible because the integrand depends only on the two independent combinations of the polar angles, i.e.,  $\tilde{\varphi}_1 = \varphi_1 - \varphi_3$  and  $\tilde{\varphi}_2 = \varphi_2 - \varphi_3$ . By using  $\tilde{\varphi}_1$  and  $\tilde{\varphi}_2$  as new integration variables (for simplicity of notation, the tildes are dropped in the following), we see that the integrand is independent



of the variable  $\varphi_3$ . Finally, by approximating  $p_1^2 p_2^2 p_3^2 \simeq \mu^6$  in the integration measure, we rewrite the expression for the rate as follows:

$$\begin{aligned} \lambda^{(\text{polar})} &\simeq \frac{5\lambda_0\mu}{2^{18}\pi^4 T} \sum_{r_1 r_2} n_{r_1} n_{r_2} \int_{-\infty}^{\infty} dx_1 \int_{-\infty}^{\infty} dx_2 \int_{-\infty}^{\infty} dx_3 \int_{-1}^1 d\xi_1 \int_{-1}^1 d\xi_2 \int_{-1}^1 d\xi_3 \int_0^{2\pi} d\varphi_1 \int_0^{2\pi} d\varphi_2 \\ &\times \frac{(1 - \cos\theta_{12})(1 - \cos\theta_{34})}{\cosh(\frac{1}{2}\epsilon_{x_1, \xi_1, r_1}) \cosh(\frac{1}{2}\epsilon_{x_2, \xi_2, r_2}) \cosh(\frac{1}{2}\epsilon_{x_3, \xi_3, r_2}) \cosh(\frac{1}{2}\epsilon_{x_4, \xi_4, r_1})} \sum_{e_1 e_2 e_3 e_4} B_{x_1, \xi_1, r_1}^{e_1} B_{x_2, \xi_2, r_2}^{e_2} B_{x_3, \xi_3, r_2}^{e_3} B_{x_4, \xi_4, r_1}^{e_4} \\ &\times \delta(e_1 \epsilon_{x_1, \xi_1, r_1} + e_2 \epsilon_{x_2, \xi_2, r_2} - e_3 \epsilon_{x_3, \xi_3, r_2} - e_4 \epsilon_{x_4, \xi_4, r_1}), \end{aligned} \quad (48)$$

where the new integration variables are  $x_i = (p_i - \mu)/T$  and  $\xi_i = \cos\theta_{\mathbf{p}_i}$ . By definition, the dimensionless energy is

$$\epsilon_{x, \xi, r} = \sqrt{x^2 + |\phi/T|^2 \lambda_{\xi, r}}, \quad (49)$$

with  $\lambda_{\xi, 1} = 1 - \xi^2$  and  $\lambda_{\xi, 2} = 0$ , and the new Bogoliubov coefficients are

$$B_{x, \xi, r}^e = \frac{1}{2} \left( 1 - e^{\frac{x}{\epsilon_{x, \xi, r}}} \right). \quad (50)$$

Note that the expressions for  $x_4$ ,  $\xi_4$  and  $\cos\theta_{34}$  in Eq. (48) are given by

$$\begin{aligned} x_4 &= \frac{p_4 - \mu}{T}, \\ \xi_4 &= \frac{p_1 \xi_1 + p_2 \xi_2 - p_3 \xi_3}{p_4}, \\ \cos\theta_{34} &= \frac{p_1 \cos\theta_{13} + p_2 \cos\theta_{23} - p_3}{p_4}, \end{aligned} \quad (51)$$

where  $p_4 = |\mathbf{p}_1 + \mathbf{p}_2 - \mathbf{p}_3|$  is a function of  $x_i$  ( $i = 1, 2, 3$ ) and the three cosine functions,

$$\begin{aligned} \cos\theta_{12} &= \xi_1 \xi_2 + \sqrt{1 - \xi_1^2} \sqrt{1 - \xi_2^2} \cos(\varphi_1 - \varphi_2), \\ \cos\theta_{13} &= \xi_1 \xi_3 + \sqrt{1 - \xi_1^2} \sqrt{1 - \xi_3^2} \cos(\varphi_1), \\ \cos\theta_{23} &= \xi_2 \xi_3 + \sqrt{1 - \xi_2^2} \sqrt{1 - \xi_3^2} \cos(\varphi_2). \end{aligned} \quad (52)$$

In the calculation, we used a customized Monte-Carlo method in order to improve the statistical error of the integration over  $x_i$  (with  $i = 1, 2, 3$ ). To this end, we used a special type of importance sampling, which is motivated by the fact that the main contribution to the rate should come from the region near the Fermi surface. In order to implement this, we utilized random variables distributed according to the Gaussian distribution [50]:

$$P(x) = \frac{1}{\sqrt{2\pi\sigma^2}} \exp\left(-\frac{(x - x_0)^2}{2\sigma^2}\right), \quad (53)$$

where  $x_0$  and  $\sigma$  are the mean and the width of the distribution, respectively. This was applied to the numerical integration over the dimensionless variables  $x_i = (p_i - \mu)/T$  ( $i = 1, 2, 3$ ), in which case we took  $x_0 = 0$

and  $\sigma = 3$ . In order to generate independent variables (e.g.,  $x_1$  and  $x_2$ ), distributed according to Eq. (53), we applied the Box-Muller transform,

$$x_1 = x_0 + \sigma \sqrt{-2 \ln u_1} \cos(2\pi u_2), \quad (54)$$

$$x_2 = x_0 + \sigma \sqrt{-2 \ln u_1} \sin(2\pi u_2), \quad (55)$$

where  $u_1$  and  $u_2$  are two independent variables, uniformly distributed in the range from 0 to 1.

In our numerical calculation, we also used a Gaussian function to approximate the  $\delta$ -function responsible for the energy conservation in the expression for the rate (48). For this purpose, we used the width of the distribution  $\sigma_0 = 0.2$ . This appeared to be sufficiently small to avoid strong violations of the energy conservation in the weak processes and, at the same time, sufficiently large to use in a Monte-Carlo integration with the number of (eight-dimensional) random points on the order of  $10^6$  (in a Mathematica code) or  $10^7$  (in a Fortran/C++ code).

The numerical results for the  $\lambda$ -rate in the polar phase are shown by the blue squares (and the interpolating line) in Fig. 3. At vanishing  $\phi/T$ , the rate coincides with that in the normal phase. At asymptotically large value of  $\phi/T$ , on the other hand, the rate approaches  $\lambda_0/9$ . This value is marked by the purple dashed line in the figure. Theoretically, the rate is dominated by the ungapped modes ( $r_1 = r_2 = 2$ ) in the  $\phi/T \rightarrow \infty$  limit. The corresponding contribution can be obtained by analytical methods as follows. We start by pointing that the Bogoliubov coefficients for the ungapped modes are equal to the unit step functions:  $B_{x_i, \xi_i, 2}^{e_i} \equiv \Theta(-e_i x_i)$ , where by definition  $\Theta(x) = 1$  for  $x \geq 0$  and  $\Theta(x) = 0$  otherwise. Since these Bogoliubov coefficients are nonzero only for  $e_i = \text{sign}(-x_i)$ , each sums over  $e_i$  effectively reduces to a single contribution. By taking this into account and making use of the result for the angular integration,  $K_0$ , defined in Appendix B, we derive

$$\begin{aligned} \lambda_{\text{unpaired}}^{(\text{polar})} &\simeq \frac{\lambda_0}{6\pi^2} \int_{-\infty}^{\infty} dx_1 \int_{-\infty}^{\infty} dx_2 \int_{-\infty}^{\infty} dx_3 \int_{-\infty}^{\infty} dx_4 \\ &\times \frac{\delta(-x_1 - x_2 + x_3 + x_4)}{(e^{x_1} + 1)(e^{x_2} + 1)(e^{-x_3} + 1)(e^{-x_4} + 1)} \\ &= \frac{1}{9} \lambda_0. \end{aligned} \quad (56)$$

It should be noted that the numerical results for the polar phase in Fig. 3 approach this asymptotic value very

slowly. We can speculate that this indicates a weak (probably, power-law) suppression of the contribution of the gapped (mixed with ungapped) modes to the rate. The key feature responsible for this behavior in the polar phase is the presence of gapless nodes at  $\theta_{\mathbf{p}} = 0$  and  $\theta_{\mathbf{p}} = \pi$  in the dispersion relation of the gapped modes. As we shall see below, the same qualitative property is shared by the *A*-phase, whose gapped modes also have a node at  $\theta_{\mathbf{p}} = \pi$ . In contrast, the rates in the CSL and planar phases, whose gapped modes have no gapless nodes, show asymptotes that are consistent with the rapid, exponential approach to their asymptotic values.

### C. Analysis of the rate in *A*-phase

The analysis in the *A*-phase of spin-one color superconducting matter can be performed along the same lines as in the polar phase. The apparent complication of the *A*-phase is the existence of three, rather than two distinct quasiparticle excitations. However, it appears that the contributions of the two gapped modes ( $r = 1, 2$ ) can be replaced by a single contribution of a modified mode with the energy  $\epsilon_{\mathbf{p}} = \sqrt{(p - \mu)^2 + |\phi|^2 \lambda_{\mathbf{p}}}$  where  $\lambda_{\mathbf{p}} \equiv (1 + \cos \theta_{\mathbf{p}})^2$  (cf. the dispersion relations of the modes  $r = 1, 2$  in Tab. I). This alternative representation is possible because of the special, separable structure of the corresponding  $\omega_{rr'}(\hat{\mathbf{p}}, \hat{\mathbf{p}}')$  functions in the *A*-phase. As seen from the expressions in Eq. (A7), the mode  $r = 1$  contributes only when  $\cos \theta_{\mathbf{p}}$  of the corresponding quasiparticle is positive, while the mode  $r = 2$  contributes only when  $\cos \theta_{\mathbf{p}}$  is negative. Then, when the contributions are nonvanishing, one always gets  $\omega_{rr'}(\hat{\mathbf{p}}, \hat{\mathbf{p}}') = 2$ . By also noting that the corresponding eigenvalues

$$\lambda_{\mathbf{p},1} = (1 + |\cos \theta_{\mathbf{p}}|)^2 \quad \text{for} \quad \cos \theta_{\mathbf{p}} > 0 \quad (57)$$

and

$$\lambda_{\mathbf{p},2} = (1 - |\cos \theta_{\mathbf{p}}|)^2 \quad \text{for} \quad \cos \theta_{\mathbf{p}} < 0 \quad (58)$$

formally take the same form, i.e.,  $\lambda_{\mathbf{p}} \equiv (1 + \cos \theta_{\mathbf{p}})^2$ , we conclude that the sum over the original modes  $r = 1, 2$  in the rate can indeed be replaced by a single contribution of the modified mode as defined above. By making use of this observation, the general expression for the rate in the *A*-phase takes the form, which is similar to that in the polar phase, see Eq. (47), but with a different dispersion relation of the (modified) gapped mode.

By using a Monte-Carlo algorithm as in the previous case, we perform a numerical calculation of the  $\lambda$ -rate in the *A*-phase. The corresponding results are shown by red stars (and the interpolating line) in Fig. 3. In the limit of large  $\phi/T$ , the rate is saturated by the contribution of ungapped modes, which is the same as in the polar phase, namely  $\lambda_0/9$ . The derivation of this asymptotic expression is the same as in the polar phase. The corresponding value is marked by the purple dashed line in the figure. A slow (probably, power-law) approach of the asymptotic

value at  $\phi/T \rightarrow \infty$  is again associated with the presence of a gapless node (at  $\theta_{\mathbf{p}} = \pi$ ) in the dispersion relation of the (modified) gapped quasiparticles.

### D. Analysis of the rate in planar phase

The calculation of the rate in the planar case requires the largest amount of computer time. One of the main reasons for that is the much more complicated expressions for the  $\omega_{rr'}(\hat{\mathbf{p}}, \hat{\mathbf{p}}')$ -functions (see Appendix A). The numerical results for the  $\lambda$ -rate in the planar phase are shown by green diamonds (and the interpolating line) in Fig. 3. The asymptotic value of the rate at large  $\phi/T$  was extracted only numerically. By taking into account possible systematic errors (e.g., due to the overall normalization of the rate that may differ by up to 15% from the analytical estimate (39) in the normal phase), we estimate  $\lambda^{(\text{planar})} \simeq (0.038 \pm 0.003)\lambda_0$  for  $\phi/T \rightarrow \infty$ . Note that this is smaller than  $\lambda_0/9$ , which is the contribution of a single mode in the normal phase. As in the CSL phase, in the planar phase the additional suppression comes from the  $\omega$ -functions for the ungapped modes.

## IV. DISCUSSION

In this paper we derived the near-equilibrium rates of the net *d*-quark production (or equivalently the  $\lambda$ -rates) due to the non-leptonic weak processes (i.e., the difference of the rates of  $u + d \rightarrow u + s$  and  $u + s \rightarrow u + d$ ) in spin-one color-superconducting strange quark matter at high density. The main numerical results are presented in Fig. 3.

In the limit of  $\phi/T = 0$ , which is same as the normal (unpaired) phase of strange quark matter, our results reproduce the known result of Ref. [47]. The effect of color superconductivity is to suppress these rates. The degree of the suppression depends on the details of the specific spin-one phases. To large extent, this is controlled by the value of the energy gap (more precisely,  $\phi/T$ ) as well as its functional dependence on the direction of the quasiparticle momentum. At very large  $\phi/T$  (or equivalently in the limit of low temperatures), the  $\lambda$ -rates approach fixed values, which are determined by the contribution of the ungapped modes alone. The corresponding limiting value is the smallest in the CSL phase. It is less than a third of the “canonical” value  $\lambda_0/9$  due to a single ungapped mode in the normal phase of matter. The additional suppression comes from the modification of the quasiparticles due to color superconductivity. A similar observation applies to the planar phase. The rates in the other two phases, i.e., the polar and *A*-phase, approach the asymptotic values equal to  $\lambda_0/9$ .

The numerical results for the  $\lambda$ -rates in Fig. 3 also indicate that the asymptotic approach to the limiting values can be qualitatively different in spin-one color superconducting phases. In the case of the polar and *A*-phase,

the approach seems to follow a power law. In contrast, the approach appears to be exponential in the case of the CSL and planar phase. This qualitative difference can be easily understood. The power law is the consequence of the presence of gapless nodes in the dispersion relations of the gapped quasiparticles in the polar and  $A$ -phase (the nodes are located at  $\theta_{\mathbf{p}} = 0$  and  $\theta_{\mathbf{p}} = \pi$  in the polar phase, and at  $\theta_{\mathbf{p}} = \pi$  in the  $A$ -phase). In the CSL and planar phase, the approach to the asymptotic value at  $\phi/T \rightarrow \infty$  is exponential because no gapless nodes are found in their gapped quasiparticles. (Note that a similar observation regarding the rates of the semi-leptonic processes was made in Ref. [36, 44].)

The results for the rates of non-leptonic weak processes, presented here, is an important ingredient for the calculation of the bulk viscosity of spin-one color-superconducting strange quark matter. If such matter is present inside neutron stars, its viscosity will be one of the mechanisms responsible for damping of the stellar  $r$ -mode instabilities [14].

### Acknowledgments

The authors would like thank Mark Alford, Prashanth Jaikumar, Armen Sedrakian, Andreas Schmitt and Qun Wang for useful comments. H.M. acknowledges discussions with Lars Zeidler. The work of I.A.S. was supported in part by the start-up funds from the Arizona State University.

## APPENDIX A: COLOR AND DIRAC TRACES

In this appendix, we write down the explicit expressions for the tensor  $\mathcal{T}_{\mu\nu}^{rr'}(\hat{\mathbf{p}}, \hat{\mathbf{p}}')$ , defined by Eq. (29). The corresponding results were obtained in Ref. [36]. In general, one finds that

$$\mathcal{T}_{r,r'}^{\mu\nu}(\hat{\mathbf{p}}, \hat{\mathbf{p}}') = \mathcal{T}^{\mu\nu}(\hat{\mathbf{p}}, \hat{\mathbf{p}}') \omega_{rr'}(\hat{\mathbf{p}}, \hat{\mathbf{p}}'), \quad (\text{A1})$$

where  $\omega_{rr'}(\hat{\mathbf{p}}, \hat{\mathbf{p}}')$  are the functions determined by a specific color-spin structure of the gap matrix, and

$$\mathcal{T}^{\mu\nu}(\hat{\mathbf{p}}, \hat{\mathbf{p}}') \equiv \text{Tr}_D \left[ \gamma^\mu (1 - \gamma^5) \gamma^0 \Lambda_{\mathbf{p}}^- \gamma^\nu (1 - \gamma^5) \gamma^0 \Lambda_{\mathbf{p}'}^- \right]. \quad (\text{A2})$$

The explicit form of all the components of this tensor can be also found in Ref. [36]. It is more important for us here to note that the following result for the contraction of this tensor with itself is valid:

$$\mathcal{T}^{\mu\nu}(\hat{\mathbf{p}}_4, \hat{\mathbf{p}}_1) \mathcal{T}_{\mu\nu}(\hat{\mathbf{p}}_3, \hat{\mathbf{p}}_2) = 16(1 - \hat{\mathbf{p}}_1 \cdot \hat{\mathbf{p}}_2)(1 - \hat{\mathbf{p}}_3 \cdot \hat{\mathbf{p}}_4). \quad (\text{A3})$$

Since an essential information regarding spin-one color-superconducting phases is carried by the  $\omega_{rr'}(\hat{\mathbf{p}}, \hat{\mathbf{p}}')$  functions, we also quote them here. (For more details, see Ref. [36].)

In the *polar* phase, the  $\omega_{rr'}(\hat{\mathbf{p}}, \hat{\mathbf{p}}')$  functions do not depend on the quark momenta. They are given by the following expressions:

$$\omega_{11}(\hat{\mathbf{p}}, \hat{\mathbf{p}}') = 2, \quad (\text{A4a})$$

$$\omega_{22}(\hat{\mathbf{p}}, \hat{\mathbf{p}}') = 1, \quad (\text{A4b})$$

$$\omega_{12}(\hat{\mathbf{p}}, \hat{\mathbf{p}}') = \omega_{21}(\hat{\mathbf{p}}, \hat{\mathbf{p}}') = 0. \quad (\text{A4c})$$

In the *planar* phase, the explicit form of the  $\omega_{rr'}(\hat{\mathbf{p}}, \hat{\mathbf{p}}')$  functions reads

$$\omega_{11}(\hat{\mathbf{p}}, \hat{\mathbf{p}}') = \frac{1}{2} [3 + \eta(\hat{\mathbf{p}}, \hat{\mathbf{p}}')], \quad (\text{A5a})$$

$$\omega_{12}(\hat{\mathbf{p}}, \hat{\mathbf{p}}') = \omega_{21}(\hat{\mathbf{p}}, \hat{\mathbf{p}}') = \frac{1}{2} [1 - \eta(\hat{\mathbf{p}}, \hat{\mathbf{p}}')], \quad (\text{A5b})$$

$$\omega_{22}(\hat{\mathbf{p}}, \hat{\mathbf{p}}') = \frac{1}{2} [1 + \eta(\hat{\mathbf{p}}, \hat{\mathbf{p}}')], \quad (\text{A5c})$$

where

$$\eta(\hat{\mathbf{p}}, \hat{\mathbf{p}}') \equiv \frac{4\hat{p}_z\hat{p}'_z + (\hat{p}_x\hat{p}'_x + \hat{p}_y\hat{p}'_y)^2 - (\hat{p}_x\hat{p}'_y - \hat{p}_y\hat{p}'_x)^2}{[1 + (\hat{p}_z)^2][1 + (\hat{p}'_z)^2]}. \quad (\text{A6})$$

In the  $A$ -phase, there are three different quasiparticle branches ( $r = 1, 2, 3$ ). Consequently, there are more  $\omega_{rr'}(\hat{\mathbf{p}}, \hat{\mathbf{p}}')$  functions, i.e.,

$$\omega_{11}(\hat{\mathbf{p}}, \hat{\mathbf{p}}') = \frac{1}{2} [1 + \text{sgn}(\hat{p}_z)][1 + \text{sgn}(\hat{p}'_z)], \quad (\text{A7a})$$

$$\omega_{22}(\hat{\mathbf{p}}, \hat{\mathbf{p}}') = \frac{1}{2} [1 - \text{sgn}(\hat{p}_z)][1 - \text{sgn}(\hat{p}'_z)], \quad (\text{A7b})$$

$$\omega_{12}(\hat{\mathbf{p}}, \hat{\mathbf{p}}') = \frac{1}{2} [1 + \text{sgn}(\hat{p}_z)][1 - \text{sgn}(\hat{p}'_z)], \quad (\text{A7c})$$

$$\omega_{21}(\hat{\mathbf{p}}, \hat{\mathbf{p}}') = \frac{1}{2} [1 - \text{sgn}(\hat{p}_z)][1 + \text{sgn}(\hat{p}'_z)], \quad (\text{A7d})$$

$$\omega_{13}(\hat{\mathbf{p}}, \hat{\mathbf{p}}') = \omega_{31}(\hat{\mathbf{p}}, \hat{\mathbf{p}}') = 0, \quad (\text{A7e})$$

$$\omega_{23}(\hat{\mathbf{p}}, \hat{\mathbf{p}}') = \omega_{32}(\hat{\mathbf{p}}, \hat{\mathbf{p}}') = 0, \quad (\text{A7f})$$

$$\omega_{33}(\hat{\mathbf{p}}, \hat{\mathbf{p}}') = 1. \quad (\text{A7g})$$

Finally, in the *CSL* phase, the corresponding functions are

$$\omega_{11}(\hat{\mathbf{p}}, \hat{\mathbf{p}}') = 1 + \frac{1}{4}(1 + \hat{\mathbf{p}} \cdot \hat{\mathbf{p}}')^2, \quad (\text{A8})$$

$$\omega_{12}(\hat{\mathbf{p}}, \hat{\mathbf{p}}') = \omega_{21}(\hat{\mathbf{p}}, \hat{\mathbf{p}}') = 1 - \frac{1}{4}(1 + \hat{\mathbf{p}} \cdot \hat{\mathbf{p}}')^2, \quad (\text{A9})$$

$$\omega_{22}(\hat{\mathbf{p}}, \hat{\mathbf{p}}') = \frac{1}{4}(1 + \hat{\mathbf{p}} \cdot \hat{\mathbf{p}}')^2. \quad (\text{A10})$$

## APPENDIX B: ANGULAR INTEGRATIONS IN CSL PHASE

In the calculation of the  $\lambda$ -rate in the CSL phase, there are four different types of angular integrations over the phase space of quark momenta. Thus, the results for the  $F_{r_1 r_2 r_3 r_4}$  functions, formally defined by Eq. (43) in the

main text, have the following general structure:

$$F_{1111} = K_0 + K_1 + K_2 + K_3, \quad (\text{B1a})$$

$$F_{1112} = K_0 - K_1 + K_2 - K_3, \quad (\text{B1b})$$

$$F_{1121} = K_0 + K_1 - K_2 - K_3, \quad (\text{B1c})$$

$$F_{1122} = K_0 - K_1 - K_2 + K_3, \quad (\text{B1d})$$

$$F_{1211} = K_0 + K_1 - K_2 - K_3, \quad (\text{B1e})$$

$$F_{1212} = K_0 - K_1 - K_2 + K_3, \quad (\text{B1f})$$

$$F_{1221} = K_2 + K_3, \quad (\text{B1g})$$

$$F_{1222} = K_2 - K_3, \quad (\text{B1h})$$

$$F_{2111} = K_0 - K_1 + K_2 - K_3, \quad (\text{B1i})$$

$$F_{2112} = K_1 + K_3, \quad (\text{B1j})$$

$$F_{2121} = K_0 - K_1 - K_2 + K_3, \quad (\text{B1k})$$

$$F_{2122} = K_1 - K_3, \quad (\text{B1l})$$

$$F_{2211} = K_0 - K_1 - K_2 + K_3, \quad (\text{B1m})$$

$$F_{2212} = K_1 - K_3, \quad (\text{B1n})$$

$$F_{2221} = K_2 - K_3, \quad (\text{B1o})$$

$$F_{2222} = K_3, \quad (\text{B1p})$$

where the four types of angular integrals are given by:

$$K_0 = \int d\Omega_1 \int d\Omega_2 \int d\Omega_3 \int d\Omega_4 (1 - \hat{\mathbf{p}}_1 \cdot \hat{\mathbf{p}}_2)(1 - \hat{\mathbf{p}}_3 \cdot \hat{\mathbf{p}}_4) \delta(\mathbf{p}_1 + \mathbf{p}_2 - \mathbf{p}_3 - \mathbf{p}_4), \quad (\text{B2})$$

$$K_1 = \frac{1}{4} \int d\Omega_1 \int d\Omega_2 \int d\Omega_3 \int d\Omega_4 (1 - \hat{\mathbf{p}}_1 \cdot \hat{\mathbf{p}}_2)(1 - \hat{\mathbf{p}}_3 \cdot \hat{\mathbf{p}}_4)(1 + \hat{\mathbf{p}}_4 \cdot \hat{\mathbf{p}}_1)^2 \delta(\mathbf{p}_1 + \mathbf{p}_2 - \mathbf{p}_3 - \mathbf{p}_4), \quad (\text{B3})$$

$$K_2 = \frac{1}{4} \int d\Omega_1 \int d\Omega_2 \int d\Omega_3 \int d\Omega_4 (1 - \hat{\mathbf{p}}_1 \cdot \hat{\mathbf{p}}_2)(1 - \hat{\mathbf{p}}_3 \cdot \hat{\mathbf{p}}_4)(1 + \hat{\mathbf{p}}_3 \cdot \hat{\mathbf{p}}_2)^2 \delta(\mathbf{p}_1 + \mathbf{p}_2 - \mathbf{p}_3 - \mathbf{p}_4), \quad (\text{B4})$$

$$K_3 = \frac{1}{16} \int d\Omega_1 \int d\Omega_2 \int d\Omega_3 \int d\Omega_4 (1 - \hat{\mathbf{p}}_1 \cdot \hat{\mathbf{p}}_2)(1 - \hat{\mathbf{p}}_3 \cdot \hat{\mathbf{p}}_4)(1 + \hat{\mathbf{p}}_4 \cdot \hat{\mathbf{p}}_1)^2 (1 + \hat{\mathbf{p}}_3 \cdot \hat{\mathbf{p}}_2)^2 \delta(\mathbf{p}_1 + \mathbf{p}_2 - \mathbf{p}_3 - \mathbf{p}_4). \quad (\text{B5})$$

The result for  $K_0$  was obtained in Ref. [25]. It reads

$$K_0 = \frac{4\pi^3}{p_1^2 p_2^2 p_3^2 p_4^2} L_0(p_{12}, P_{12}, p_{34}, P_{34}), \quad (\text{B6})$$

where  $p_{ij} \equiv |p_i - p_j|$ ,  $P_{ij} \equiv p_i + p_j$ , and

$$\begin{aligned} L_0(a, b, c, d) &\equiv \Theta(c - a)\Theta(d - b)\Theta(b - c)J_0(c, b, b, d) + \Theta(a - c)\Theta(d - b)J_0(a, b, b, d) \\ &+ \Theta(a - c)\Theta(b - d)\Theta(d - a)J_0(a, d, b, d) + \Theta(c - a)\Theta(b - d)J_0(c, d, b, d), \end{aligned} \quad (\text{B7})$$

which is given in terms of

$$J_0(a, b, c, d) \equiv \int_a^b dP (c^2 - P^2)(d^2 - P^2) = c^2 d^2 (b - a) - \frac{1}{3}(c^2 + d^2)(b^3 - a^3) + \frac{1}{5}(b^5 - a^5). \quad (\text{B8})$$

To leading order in powers of large  $\mu$ , this result simplifies to

$$L_0(0, 2\mu, 0, 2\mu) = \frac{2^8 \mu^5}{15}. \quad (\text{B9})$$

By making use of Eq. (B6), therefore, we obtain

$$K_0 \simeq \frac{4\pi^3}{\mu^8} L_0(0, 2\mu, 0, 2\mu) = \frac{2^{10} \pi^3}{15 \mu^3}. \quad (\text{B10})$$

Using the same approach, in the following subsections we calculate the results for  $K_1$ ,  $K_2$ , and  $K_3$ .

### 1. Calculation of $K_1$

Here we calculate the angular integral  $K_1$ . Following the approach of Ref. [25], we obtain

$$\begin{aligned}
K_1 &= \frac{1}{4} \int d\Omega_1 \int d\Omega_2 \int d\Omega_3 \int d\Omega_4 (1 - \hat{\mathbf{p}}_1 \cdot \hat{\mathbf{p}}_2)(1 - \hat{\mathbf{p}}_3 \cdot \hat{\mathbf{p}}_4)(1 + \hat{\mathbf{p}}_4 \cdot \hat{\mathbf{p}}_1)^2 \delta(\mathbf{p}_1 + \mathbf{p}_2 - \mathbf{p}_3 - \mathbf{p}_4) \\
&= \frac{1}{4p_2^2} \int d\Omega_1 \int d\Omega_3 \int d\Omega_4 \left[ 1 - \frac{1}{p_2} (\hat{\mathbf{p}}_1 \cdot \mathbf{P} - p_1) \right] (1 - \hat{\mathbf{p}}_3 \cdot \hat{\mathbf{p}}_4)(1 + \hat{\mathbf{p}}_4 \cdot \hat{\mathbf{p}}_1)^2 \delta(p_2 - |\mathbf{P} - \mathbf{p}_1|) \\
&= \frac{1}{4p_2^2} \int d\Omega_3 \int d\Omega_4 \int_0^{2\pi} d\phi_1 \int_0^\pi d\theta_1 \sin \theta_1 \left[ 1 - \frac{1}{p_2} (P \cos \theta_1 - p_1) \right] (1 - \hat{\mathbf{p}}_3 \cdot \hat{\mathbf{p}}_4) \delta(p_2 - |\mathbf{P} - \mathbf{p}_1|) \\
&\quad \times [1 + \cos \theta_1 \cos \theta_4 + \sin \theta_1 \sin \theta_4 \cos(\phi_1 - \phi_4)]^2, \tag{B11}
\end{aligned}$$

where  $\mathbf{P} = \mathbf{p}_3 + \mathbf{p}_4$  and  $P = |\mathbf{P}|$ . In order to integrate over  $\theta_1$ , we choose the coordinate system so that the  $z$ -axis is along the vector  $\mathbf{P}$ . After making use of the  $\delta$ -function, we easily integrate over  $\theta_1$  and arrive at the following result:

$$\begin{aligned}
K_1 &= \int d\Omega_3 \int d\Omega_4 \frac{P_{12}^2 - P^2}{8Pp_1^2p_2^2} (1 - \hat{\mathbf{p}}_3 \cdot \hat{\mathbf{p}}_4) \Theta(P_{12} - P) \Theta(P - p_{12}) \\
&\quad \times \int_0^{2\pi} d\phi_1 [1 + \cos \theta_1^* \cos \theta_4 + \sin \theta_1^* \sin \theta_4 \cos(\phi_1 - \phi_4)]^2 \\
&= \pi \int d\Omega_3 \int d\Omega_4 \frac{P_{12}^2 - P^2}{8Pp_1^2p_2^2} \Theta(P_{12} - P) \Theta(P - p_{12}) (1 - \hat{\mathbf{p}}_3 \cdot \hat{\mathbf{p}}_4) \left[ 2(1 + \cos \theta_1^* \cos \theta_4)^2 + (\sin \theta_1^* \sin \theta_4)^2 \right] \tag{B12}
\end{aligned}$$

where  $\cos \theta_1^* = (P^2 + p_1^2 - p_2^2)/2Pp_1$  and  $\cos \theta_4 = (\hat{\mathbf{p}}_4 \cdot \hat{\mathbf{P}}) = (P^2 + p_4^2 - p_3^2)/2Pp_4$ . It may be appropriate to emphasize that the result of the last integration was presented in a form that independent of a specific choice of the coordinate system. As can be easily checked, the integrand in Eq. (B12) depends only on the relative angle  $\theta_{34}$  between the vectors  $\hat{\mathbf{p}}_3$  and  $\hat{\mathbf{p}}_4$  (or equivalently only on the variable  $P$ ). Therefore, while integrating over  $\Omega_4$ , we could fix the orientation of  $\hat{\mathbf{p}}_3$  arbitrarily. It is convenient to choose  $\hat{\mathbf{p}}_3$  as the  $z$ -axis and perform the integration over  $\Omega_4$ . The result is independent of the angular coordinates in  $\Omega_3$ . Thus, the remaining integration over  $\Omega_3$  gives an extra factor  $4\pi$ . In the end, we arrive at

$$K_1 = \frac{\pi^3}{2p_1^2p_2^2p_3^2p_4^2} \int_{p_{34}}^{P_{34}} g(P) dP, \tag{B13}$$

where

$$\begin{aligned}
g(P) &= (P_{12}^2 - P^2)(P_{34}^2 - P^2) \Theta(P_{12} - P) \Theta(P - p_{12}) \left[ 2 \left( 1 + \frac{(P^2 + p_1^2 - p_2^2)(P^2 + p_4^2 - p_3^2)}{4P^2p_1p_4} \right)^2 \right. \\
&\quad \left. + \left( 1 - \frac{(P^2 + p_1^2 - p_2^2)^2}{4P^2p_1^2} \right) \left( 1 - \frac{(P^2 + p_4^2 - p_3^2)^2}{4P^2p_4^2} \right) \right]. \tag{B14}
\end{aligned}$$

Note that we changed the integration variable from  $\theta_{34}$  to  $P = \sqrt{p_3^2 + p_4^2 + 2p_3p_4 \cos \theta_{34}}$ .

The final result for  $K_1$  can be conveniently given in the same form as  $K_0$  in the previous section, i.e.,

$$K_1 = \frac{\pi^3}{2p_1^2p_2^2p_3^2p_4^2} L_1(p_{12}, P_{12}, p_{34}, P_{34}), \tag{B15}$$

where, by definition,

$$\begin{aligned}
L_1(a, b, c, d) &\equiv \Theta(c - a) \Theta(d - b) \Theta(b - c) J_1(c, b, b, d) + \Theta(a - c) \Theta(d - b) J_1(a, b, b, d) \\
&\quad + \Theta(a - c) \Theta(b - d) \Theta(d - a) J_1(a, d, b, d) + \Theta(c - a) \Theta(b - d) J_1(c, d, b, d), \tag{B16}
\end{aligned}$$

and

$$\begin{aligned}
J_1(a, b, c, d) &= \int_a^b dP (c^2 - P^2)(d^2 - P^2) \left[ 2 \left( 1 + \frac{(P^2 + p_1^2 - p_2^2)(P^2 + p_4^2 - p_3^2)}{4P^2p_1p_4} \right)^2 \right. \\
&\quad \left. + \left( 1 - \frac{(P^2 + p_1^2 - p_2^2)^2}{4P^2p_1^2} \right) \left( 1 - \frac{(P^2 + p_4^2 - p_3^2)^2}{4P^2p_4^2} \right) \right]. \tag{B17}
\end{aligned}$$



To leading order in powers of large  $\mu$ , this result reduces to

$$L_1(0, 2\mu, 0, 2\mu) = \frac{2^{11}\mu^5}{35}. \quad (\text{B18})$$

This, in turn, gives

$$K_1 \simeq \frac{\pi^3}{2\mu^8} L_1(0, 2\mu, 0, 2\mu) = \frac{2^{10}\pi^3}{35\mu^3}. \quad (\text{B19})$$

## 2. Calculation of $K_2$

As is easy to see, the expression for  $K_2$  can be obtained from  $K_1$  by the following exchange of variables:  $p_1 \leftrightarrow p_2$  and  $p_3 \leftrightarrow p_4$ . Thus, the result reads

$$K_2 = \frac{\pi^3}{2p_1^2 p_2^2 p_3^2 p_4^2} L_2(p_{12}, P_{12}, p_{34}, P_{34}), \quad (\text{B20})$$

where

$$\begin{aligned} L_2(a, b, c, d) \equiv & \Theta(c-a)\Theta(d-b)\Theta(b-c)J_2(c, b, b, d) + \Theta(a-c)\Theta(d-b)J_2(a, b, b, d) \\ & + \Theta(a-c)\Theta(b-d)\Theta(d-a)J_2(a, d, b, d) + \Theta(c-a)\Theta(b-d)J_2(c, d, b, d), \end{aligned} \quad (\text{B21})$$

and

$$\begin{aligned} J_2(a, b, c, d) = & \int_a^b dP (c^2 - P^2)(d^2 - P^2) \left[ 2 \left( 1 + \frac{(P^2 + p_2^2 - p_1^2)(P^2 + p_3^2 - p_4^2)}{4P^2 p_2 p_3} \right)^2 \right. \\ & \left. + \left( 1 - \frac{(P^2 + p_2^2 - p_1^2)^2}{4P^2 p_2^2} \right) \left( 1 - \frac{(P^2 + p_3^2 - p_4^2)^2}{4P^2 p_3^2} \right) \right]. \end{aligned} \quad (\text{B22})$$

We also find that  $K_2$  is identical to  $K_1$  to leading order in powers of large  $\mu$ , i.e.,

$$K_2 \simeq \frac{2^{10}\pi^3}{35\mu^3}. \quad (\text{B23})$$

## 3. Calculation of $K_3$

Now we calculate the angular integral  $K_3$ . We start by using the same approach as in the calculation of  $K_1$ ,

$$\begin{aligned} K_3 = & \frac{1}{16p_2^2} \int d\Omega_1 \int d\Omega_3 \int d\Omega_4 \left[ 1 - \frac{1}{p_2} (\hat{\mathbf{p}}_1 \cdot \mathbf{P} - p_1) \right] (1 - \hat{\mathbf{p}}_3 \cdot \hat{\mathbf{p}}_4) (1 + \hat{\mathbf{p}}_4 \cdot \hat{\mathbf{p}}_1)^2 \\ & \times \left[ 1 + \frac{1}{p_2 p_3} (\mathbf{p}_3 \cdot \mathbf{P} - \mathbf{p}_1 \cdot \mathbf{P} + \mathbf{p}_1 \cdot \mathbf{p}_4) \right]^2 \delta(p_2 - |\mathbf{P} - \mathbf{p}_1|). \end{aligned} \quad (\text{B24})$$

To calculate the integral over  $\Omega_1$ , we fix the coordinate system so that the z-axis coincides with the direction of  $\mathbf{P}$ . After integration, we obtain

$$\begin{aligned} K_3 = & \int d\Omega_3 \int d\Omega_4 \frac{P_{12}^2 - P^2}{32P p_1^2 p_2^2} \Theta(P_{12} - P) \Theta(P - p_{12}) (1 - \hat{\mathbf{p}}_3 \cdot \hat{\mathbf{p}}_4) \\ & \times \int_0^{2\pi} d\phi_1 [1 + \cos \theta_1^* \cos \theta_4 + \sin \theta_1^* \sin \theta_4 \cos(\phi_1 - \phi_4)]^2 \\ & \times \left[ 1 + \frac{p_2^2 - p_1^2 + p_3^2 - p_4^2}{2p_2 p_3} + \frac{p_1 p_4}{p_2 p_3} (\cos \theta_1^* \cos \theta_4 + \sin \theta_1^* \sin \theta_4 \cos(\phi_1 - \phi_4)) \right]^2, \end{aligned} \quad (\text{B25})$$

where  $\cos \theta_1^* = (P^2 + p_1^2 - p_2^2)/2Pp_1$  and  $\cos \theta_4 = (\hat{\mathbf{p}}_4 \cdot \hat{\mathbf{P}}) = (P^2 + p_4^2 - p_3^2)/2Pp_4$ . In the derivation, we also used the following relation:

$$\mathbf{p}_3 \cdot \mathbf{P} = \frac{P^2 + p_3^2 - p_4^2}{2}. \quad (\text{B26})$$

By performing the integration over  $\phi_1$ , we derive

$$\begin{aligned} K_3 = & \pi \int d\Omega_3 \int d\Omega_4 \frac{(P_{12}^2 - P^2)(P_{34}^2 - P^2)}{256Pp_1^2p_2^2p_3^2p_4^2} \Theta(P_{12} - P) \Theta(P - p_{12}) \\ & \times \left\{ (P_{14}^2 - P_{23}^2)^2 \left[ 2 \left( 1 + \frac{(P^2 + p_1^2 - p_2^2)(P^2 + p_4^2 - p_3^2)}{4P^2p_1p_4} \right)^2 + \left( 1 - \frac{(P^2 + p_1^2 - p_2^2)^2}{4P^2p_1^2} \right) \left( 1 - \frac{(P^2 + p_4^2 - p_3^2)^2}{4P^2p_4^2} \right) \right] \right. \\ & - 4p_1p_4 (P_{14}^2 - P_{23}^2) \left( 1 + \frac{(P^2 + p_1^2 - p_2^2)(P^2 + p_4^2 - p_3^2)}{4P^2p_1p_4} \right) \\ & \times \left[ 2 \left( 1 + \frac{(P^2 + p_1^2 - p_2^2)(P^2 + p_4^2 - p_3^2)}{4P^2p_1p_4} \right)^2 + 3 \left( 1 - \frac{(P^2 + p_1^2 - p_2^2)^2}{4P^2p_1^2} \right) \left( 1 - \frac{(P^2 + p_4^2 - p_3^2)^2}{4P^2p_4^2} \right) \right] \\ & + p_1^2p_4^2 \left[ 8 \left( 1 + \frac{(P^2 + p_1^2 - p_2^2)(P^2 + p_4^2 - p_3^2)}{4P^2p_1p_4} \right)^4 + 3 \left( 1 - \frac{(P^2 + p_1^2 - p_2^2)^2}{4P^2p_1^2} \right)^2 \left( 1 - \frac{(P^2 + p_4^2 - p_3^2)^2}{4P^2p_4^2} \right)^2 \right. \\ & \left. \left. + 24 \left( 1 + \frac{(P^2 + p_1^2 - p_2^2)(P^2 + p_4^2 - p_3^2)}{4P^2p_1p_4} \right)^2 \left( 1 - \frac{(P^2 + p_1^2 - p_2^2)^2}{4P^2p_1^2} \right) \left( 1 - \frac{(P^2 + p_4^2 - p_3^2)^2}{4P^2p_4^2} \right) \right] \right\}, \quad (\text{B27}) \end{aligned}$$

Finally, in order to integrating over  $\Omega_4$ , we use the coordinate system with the z-axis along  $\hat{\mathbf{p}}_3$ . Then, we get

$$K_3 = \frac{\pi^3}{32p_1^2p_2^2p_3^2p_4^2} \int_{p_{34}}^{P_{34}} h(P) dP, \quad (\text{B28})$$

where

$$\begin{aligned} h(P) = & (P_{12}^2 - P^2)(P_{34}^2 - P^2) \Theta(P_{12} - P) \Theta(P - p_{12}) \\ & \times \left\{ (P_{14}^2 - P_{23}^2)^2 \left[ 2 \left( 1 + \frac{(P^2 + p_1^2 - p_2^2)(P^2 + p_4^2 - p_3^2)}{4P^2p_1p_4} \right)^2 + \left( 1 - \frac{(P^2 + p_1^2 - p_2^2)^2}{4P^2p_1^2} \right) \left( 1 - \frac{(P^2 + p_4^2 - p_3^2)^2}{4P^2p_4^2} \right) \right] \right. \\ & - 4p_1p_4 (P_{14}^2 - P_{23}^2) \left( 1 + \frac{(P^2 + p_1^2 - p_2^2)(P^2 + p_4^2 - p_3^2)}{4P^2p_1p_4} \right) \\ & \times \left[ 2 \left( 1 + \frac{(P^2 + p_1^2 - p_2^2)(P^2 + p_4^2 - p_3^2)}{4P^2p_1p_4} \right)^2 + 3 \left( 1 - \frac{(P^2 + p_1^2 - p_2^2)^2}{4P^2p_1^2} \right) \left( 1 - \frac{(P^2 + p_4^2 - p_3^2)^2}{4P^2p_4^2} \right) \right] \\ & + p_1^2p_4^2 \left[ 8 \left( 1 + \frac{(P^2 + p_1^2 - p_2^2)(P^2 + p_4^2 - p_3^2)}{4P^2p_1p_4} \right)^4 + 3 \left( 1 - \frac{(P^2 + p_1^2 - p_2^2)^2}{4P^2p_1^2} \right)^2 \left( 1 - \frac{(P^2 + p_4^2 - p_3^2)^2}{4P^2p_4^2} \right)^2 \right. \\ & \left. \left. + 24 \left( 1 + \frac{(P^2 + p_1^2 - p_2^2)(P^2 + p_4^2 - p_3^2)}{4P^2p_1p_4} \right)^2 \left( 1 - \frac{(P^2 + p_1^2 - p_2^2)^2}{4P^2p_1^2} \right) \left( 1 - \frac{(P^2 + p_4^2 - p_3^2)^2}{4P^2p_4^2} \right) \right] \right\}. \quad (\text{B29}) \end{aligned}$$

The result can be given in the same form as the other integrals in the previous subsections, i.e.,

$$K_3 = \frac{\pi^3}{32p_1^2p_2^2p_3^2p_4^2} L_3(p_{12}, P_{12}, p_{34}, P_{34}), \quad (\text{B30})$$

where

$$\begin{aligned} L_3(a, b, c, d) \equiv & \Theta(c - a) \Theta(d - b) \Theta(b - c) J_3(c, b, b, d) + \Theta(a - c) \Theta(d - b) J_3(a, b, b, d) \\ & + \Theta(a - c) \Theta(b - d) \Theta(d - a) J_3(a, d, b, d) + \Theta(c - a) \Theta(b - d) J_3(c, d, b, d), \quad (\text{B31}) \end{aligned}$$

and

$$\begin{aligned}
J_3(a, b, c, d) = & \int_a^b dP (c^2 - P^2)(d^2 - P^2) \left\{ (P_{14}^2 - P_{23}^2)^2 \right. \\
& \times \left[ 2 \left( 1 + \frac{(P^2 + p_1^2 - p_2^2)(P^2 + p_4^2 - p_3^2)}{4P^2 p_1 p_4} \right)^2 + \left( 1 - \frac{(P^2 + p_1^2 - p_2^2)^2}{4P^2 p_1^2} \right) \left( 1 - \frac{(P^2 + p_4^2 - p_3^2)^2}{4P^2 p_4^2} \right) \right] \\
& - 4p_1 p_4 (P_{14}^2 - P_{23}^2) \left( 1 + \frac{(P^2 + p_1^2 - p_2^2)(P^2 + p_4^2 - p_3^2)}{4P^2 p_1 p_4} \right) \\
& \times \left[ 2 \left( 1 + \frac{(P^2 + p_1^2 - p_2^2)(P^2 + p_4^2 - p_3^2)}{4P^2 p_1 p_4} \right)^2 + 3 \left( 1 - \frac{(P^2 + p_1^2 - p_2^2)^2}{4P^2 p_1^2} \right) \left( 1 - \frac{(P^2 + p_4^2 - p_3^2)^2}{4P^2 p_4^2} \right) \right] \\
& + p_1^2 p_4^2 \left[ 8 \left( 1 + \frac{(P^2 + p_1^2 - p_2^2)(P^2 + p_4^2 - p_3^2)}{4P^2 p_1 p_4} \right)^4 + 3 \left( 1 - \frac{(P^2 + p_1^2 - p_2^2)^2}{4P^2 p_1^2} \right)^2 \left( 1 - \frac{(P^2 + p_4^2 - p_3^2)^2}{4P^2 p_4^2} \right)^2 \right. \\
& \left. \left. + 24 \left( 1 + \frac{(P^2 + p_1^2 - p_2^2)(P^2 + p_4^2 - p_3^2)}{4P^2 p_1 p_4} \right)^2 \left( 1 - \frac{(P^2 + p_1^2 - p_2^2)^2}{4P^2 p_1^2} \right) \left( 1 - \frac{(P^2 + p_4^2 - p_3^2)^2}{4P^2 p_4^2} \right) \right] \right\}. \quad (\text{B32})
\end{aligned}$$

To leading order in powers of large  $\mu$ , the result reduces to

$$L_3(0, 2\mu, 0, 2\mu) = \frac{29 \times 2^{20} \mu^9}{45045}. \quad (\text{B33})$$

Then, by making use of the relation in Eq. (B30), we derive

$$K_3 \simeq \frac{\pi^3}{2\mu^{12}} L_3(0, 2\mu, 0, 2\mu) = \frac{29 \times 2^{15} \pi^3}{45045 \mu^3}. \quad (\text{B34})$$

#### 4. $F_{r_1 r_2 r_3 r_4}$ to leading order in inverse powers of $\mu$

By making use of the leading order results for  $K_i$  ( $i = 1, 2, 3$ ) obtained in the previous subsections, here we write down the explicit results for the functions  $F_{r_1 r_2 r_3 r_4}$  in the same approximation:

$$F_{1111} = \frac{1301 \times 2^{10} \pi^3}{9009 \mu^3}, \quad (\text{B35a})$$

$$F_{1221} = F_{2112} = \frac{443 \times 2^{10} \pi^3}{9009 \mu^3}, \quad (\text{B35b})$$

$$F_{1112} = F_{1121} = F_{1211} = F_{2111} = \frac{415 \times 2^{10} \pi^3}{9009 \mu^3}, \quad (\text{B35c})$$

$$F_{1122} = F_{1212} = F_{2121} = F_{2211} = \frac{1357 \times 2^{10} \pi^3}{45045 \mu^3}, \quad (\text{B35d})$$

$$F_{1222} = F_{2122} = F_{2212} = F_{2221} = \frac{359 \times 2^{10} \pi^3}{45045 \mu^3}, \quad (\text{B35e})$$

$$F_{2222} = \frac{29 \times 2^{15} \pi^3}{45045 \mu^3}. \quad (\text{B35f})$$

Note that

$$\sum_{r_1, r_2, r_3, r_4} F_{r_1 r_2 r_3 r_4} = \frac{3 \times 2^{10} \pi^3}{5 \mu^3}. \quad (\text{B36})$$

- 
- [1] J. C. Collins and M. J. Perry, Phys. Rev. Lett. **34**, 1353 (1975).
  - [2] B. C. Barrois, Nucl. Phys. B **129**, 390 (1977).
  - [3] D. Bailin and A. Love, Phys. Lett. B **137**, 348 (1984).
  - [4] K. Rajagopal and F. Wilczek, arXiv:hep-ph/0011333.
  - [5] M. G. Alford, Ann. Rev. Nucl. Part. Sci. **51** (2001) 131.
  - [6] D. K. Hong, Acta Phys. Polon. B **32**, 1253 (2001).
  - [7] D. H. Rischke, Prog. Part. Nucl. Phys. **52**, 197 (2004).
  - [8] S. Reddy, Acta Phys. Polon. B **33**, 4101 (2002).
  - [9] M. Buballa, Phys. Rept. **407**, 205 (2005).
  - [10] I. A. Shovkovy, Found. Phys. **35**, 1309 (2005).
  - [11] M. G. Alford, A. Schmitt, K. Rajagopal and T. Schäfer, Rev. Mod. Phys. **80**, 1455 (2008).
  - [12] Q. Wang, arXiv:0912.2485 [nucl-th].
  - [13] N. Iwamoto, Phys. Rev. Lett. **44**, 1637 (1980).
  - [14] N. Andersson, Astrophys. J. **502**, 708 (1998).
  - [15] J. Madsen, Phys. Rev. Lett. **81**, 3311 (1998).
  - [16] M. G. Alford, K. Rajagopal and F. Wilczek, Nucl. Phys. B **537**, 443 (1999).
  - [17] P. Jaikumar, M. Prakash and T. Schäfer, Phys. Rev. D **66**, 063003 (2002).
  - [18] S. Reddy, M. Sadzikowski and M. Tachibana, Nucl. Phys. A **714**, 337 (2003).
  - [19] M. G. Alford, M. Braby, S. Reddy and T. Schäfer, Phys. Rev. C **75**, 055209 (2007); M. G. Alford, M. Braby and A. Schmitt, J. Phys. G **35**, 115007 (2008).
  - [20] P. Jaikumar, G. Rupak and A. W. Steiner, Phys. Rev. D **78**, 123007 (2008).

- [21] M. G. Alford, M. Braby and S. Mahmoodifar, arXiv:0910.2180 [nucl-th].
- [22] M. Alford and K. Rajagopal, JHEP **0206**, 031 (2002).
- [23] M. Alford, K. Rajagopal, and F. Wilczek, Phys. Lett. B **422**, 247 (1998); R. Rapp, T. Schäfer, E. V. Shuryak, and M. Velkovsky, Phys. Rev. Lett. **81**, 53 (1998).
- [24] P. Jaikumar, C. D. Roberts and A. Sedrakian, Phys. Rev. C **73**, 042801 (2006)
- [25] M. G. Alford and A. Schmitt, J. Phys. G **34**, 67 (2007).
- [26] M. G. Alford, J. A. Bowers and K. Rajagopal, Phys. Rev. D **63**, 074016 (2001); J.A. Bowers and K. Rajagopal, Phys. Rev. D **66**, 065002 (2002); K. Rajagopal and R. Sharma, Phys. Rev. D **74**, 094019 (2006); A. Sedrakian and D. H. Rischke, Phys. Rev. D **80**, 074022 (2009).
- [27] I. Shovkovy and M. Huang, Phys. Lett. B **564**, 205 (2003).
- [28] M. Alford, C. Kouvaris and K. Rajagopal, Phys. Rev. Lett. **92**, 222001 (2004).
- [29] P.F. Bedaque and T. Schäfer, Nucl. Phys. A **697**, 802 (2002); D.B. Kaplan and S. Reddy, Phys. Rev. D **65**, 054042 (2002); T. Schäfer, Phys. Rev. Lett. **96**, 012305 (2006); A. Kryjevski, Phys. Rev. D **77**, 014018 (2008).
- [30] E.V. Gorbar, M. Hashimoto, and V.A. Miransky, Phys. Lett. B **632**, 305 (2006); Phys. Rev. D **75**, 085012 (2007).
- [31] T. Schäfer, Phys. Rev. D **62**, 094007 (2000).
- [32] A. Schmitt, Phys. Rev. D **71**, 054016 (2005).
- [33] M. G. Alford, J. A. Bowers, J. M. Cheyne, and G. A. Cowan, Phys. Rev. D **67**, 054018 (2003).
- [34] A. Schmitt, Q. Wang, and D. H. Rischke, Phys. Rev. Lett. **91**, 242301 (2003).
- [35] T. Brauner, Phys. Rev. D **78**, 125027 (2008); T. Brauner, J. Y. Pang and Q. Wang, arXiv:0909.4201 [hep-ph].
- [36] A. Schmitt, I. A. Shovkovy and Q. Wang, Phys. Rev. D **73**, 034012 (2006).
- [37] Q. D. Wang and T. Lu, Phys. Lett. **148B**, 211 (1984).
- [38] R. F. Sawyer, Phys. Lett. B **233**, 412 (1989).
- [39] J. Madsen, Phys. Rev. D **46**, 3290 (1992).
- [40] Z. Xiaoping, L. Xuewen, K. Miao, and Y. Shuhua, Phys. Rev. C **70**, 015803 (2004); Z. Xiaoping, K. Miao, L. Xuewen, and Y. Shuhua, Phys. Rev. C **72**, 025809 (2005).
- [41] X.-p. Zheng, S.-h. Yang, and J.-R. Li, Phys. Lett. B **548**, 29 (2002).
- [42] H. Dong, N. Su and Q. Wang, Phys. Rev. D **75**, 074016 (2007); J. Phys. G **34**, S643 (2007)
- [43] B. A. Sa'd, I. A. Shovkovy and D. H. Rischke, Phys. Rev. D **75**, 125004 (2007).
- [44] B. A. Sa'd, I. A. Shovkovy and D. H. Rischke, Phys. Rev. D **75**, 065016 (2007).
- [45] A. Sedrakian and A. E. L. Dieperink, Phys. Rev. D **62**, 083002 (2000); A. Sedrakian, Phys. Lett. B **607**, 27 (2005); A. Sedrakian, Prog. Part. Nucl. Phys. **58**, 168 (2007).
- [46] L. P. Kadanoff and G. Baym, *Quantum Statistical Mechanics* (Benjamin, New York, 1962).
- [47] J. Madsen, Phys. Rev. D **47**, 325 (1993).
- [48] Note, however, that the rate at zero temperature is cubic in  $\delta\mu$  [47]:  $\Gamma_d \simeq (16/5\pi^5)G_F^2 V_{us}^2 V_{ud}^2 \mu^5 \delta\mu^3$ .
- [49] See EPAPS supplementary material at [URL will be inserted by AIP] for the data files containing the normalized values of the  $\lambda$ -rates.
- [50] S. Weinzierl, arXiv:hep-ph/0006269.